High Resolution Quantitative Auto-Radiography to Determine Microscopic Distributions of B-10 in Neutron Capture Therapy

By

Thomas C. Harris

B.A. Physics, B.A. German Studies, Dartmouth College (2000)

Submitted to the Department of Nuclear Science and Engineering
in Partial Fulfillment of the Requirements for the Degree of

Master of Science in Nuclear Science and Engineering

At the

Massachusetts Institute of Technology

June 2006

Signature of Author _____
Department of Nuclear Science and Engineering
May 12, 2006

Certified by _____
Otto K. Harling
Professor of Nuclear Science and Engineering
Thesis Supervisor

_____
Jeffrey A. Coderre
Associate Professor of Nuclear Science and Engineering
Co-Thesis Supervisor

Accepted by _____
Jeffrey A. Coderre
Associate Professor of Nuclear Science and Engineering
Chairman, Department Committee on Graduate Students

High Resolution Quantitative Auto-Radiography to Determine Microscopic Distributions of B-10 in Neutron Capture Therapy

By

Thomas C. Harris

Submitted to the Department of Nuclear Science and Engineering on May 12, 2006 in Partial Fulfillment of the Requirements for the Degree of Master of Science in Nuclear Science and Engineering

Abstract

The success of Boron Neutron Capture Therapy (BNCT) is heavily dependent on the microscopic distribution of B-10 in tissue. High Resolution Quantitative Auto-Radiography (HRQAR) is a potentially valuable analytical tool due to its ability to simultaneously visualize boron distributions and tissue histology. While powerful, the technique has fallen into disuse, largely due to its complexity.

HRQAR was reconstituted, and its accuracy was verified with test samples. Numerous improvements were made to make the process easier and more efficient. Permanent staff members at the Institute were trained in the technique, ensuring the continued vitality of HRQAR.

The image acquisition equipment and analysis software were modernized, and made more user-friendly. The microdosimetry analysis software was updated to current versions of programming environments and personal computer operating systems. Verification tests were conducted to ensure the continued accuracy of the underlying algorithms.

Several experiments were conducted to demonstrate the applications of HRQAR. One focus of current BNCT research is the development of new boron delivery agents, so a potential new compound was compared with a current-generation boron compound. In order to underscore the broader range of utility of HRQAR, another experiment was conducted using the auto-radiography technique as verification of selective microvasculature irradiation.

Thesis Supervisor: Otto K. Harling
Title: Professor of Nuclear Science and Engineering

Thesis Co-Supervisor: Jeffrey A. Coderre
Title: Associate Professor Nuclear Science and Engineering

Acknowledgements

I would like to thank my thesis supervisors, Professor Otto Harling and Professor Jeffrey Coderre, for their wisdom and guidance over the years. The opportunity to work on such an interesting project is very much appreciated. I would also like to thank Stead Kiger for his assistance in helping solve the countless problems I had getting started with the technique.

Kent Riley and Peter Binns were both exceptionally helpful. In particular, their experience and advice on day-to-day matters in the lab helped make me a more effective and efficient researcher. They also made themselves readily available to operate the M-011 medical thermal neutron beam. Hemant Patel lent me some of his considerable expertise in biology techniques, in which I had zero experience when I started.

My fellow graduate students, Brad Schuller and Yoonsun Chung, I would like to thank for all the long chats – professional and otherwise – that contributed to the project and helped keep me sane, respectively. They also happily took care of all animal husbandry matters, for which my squeamish stomach is eternally grateful. I would like to thank Frank Warmsley, my ever dauntless and patient reactor operator, for his immeasurable help and feedback in performing 3GV irradiations. Judy Maro of reactor operations somehow made dealing with the logistics of a research reactor a charming snap. Carolyn Dulong, our office's skilled administrative assistant, always had a cheerful smile and a pleasant chat handy, even as I brought her yet *another* purchase slip to process.

My family has been there for me the whole time, supporting me through the tough times, and cheering me on for the good. Their obvious love for me is a source of strength I have drawn on over the years. And last but most certainly not least, I would like to thank my "Ferret." Companion, confidant, psychotherapist (and copy editor) she means everything to me. I would not be a fraction of the person I am without her. I feel truly blessed to have such wonderful people supporting me.

Table of Contents

Chapter 1
Introduction

1.1 Boron Neutron Capture Therapy

Boron Neutron Capture Therapy (BNCT) is a binary cancer therapy which has been tested principally in the treatment of highly refractory cancers: the brain tumor glioblastoma multiforme and metastatic melanoma. Studies of applications to other cancers, such as head & neck[1] and lung, are also underway. A boron-10 containing compound is administered to the patient, accumulating preferentially in tumor sites. The treatment site is then irradiated with a neutron beam, inducing the $^{10}B(n,\alpha)^{7}Li$ capture reaction. The alpha particle and lithium ions have a combined range of about one cell diameter, confining the ^{10}B component of the dose largely to tumor cells, sparing the surrounding healthy tissue.

Achieving cell kill with densely ionizing radiation is typically accomplished by dealing direct damage to the cell's DNA, creating a double strand break. The alpha particle and lithium ion have initial core radii of 0.00065 and 0.00019 microns[2], and track lengths of 7 and 4 microns, respectively, meaning that only a small fraction of the cell volume is damaged. In order to assess the effectiveness of a boron compound, the extent of boron accumulation in tumor cells as well as the intracellular distribution of the boron must be determined. A boron capture reaction occurring in a cell nucleus is much more likely to result in cell death than a capture reaction in the cell's cytoplasm.[3]

1.2 Goals

The primary goal of this thesis is to implement an imaging technique that permits analysis of the intracellular distribution of boron on a histological sample, and to make improvements in its capabilities and its ease-of-use, where possible. High Resolution Quantitative Auto-Radiography (HRQAR) permits such boron visualization, with a resolution of 1 micron. The technique was implemented most recently at MIT[4], however, due to its difficulty and absence of continuity in staffing, HRQAR had fallen into disuse. Chapter 2 details the procedure for preparing and irradiating tissue samples. Chapter 3 discusses obtaining and analyzing HRQAR images. Chapter 4 provides the reader with a user guide to the microdosimetry analysis software used to quantify the images. Chapter 5 presents experimental data obtained via HRQAR comparing a standard neutron capture therapy compound with a potential liposomal compound undergoing initial evaluation. Chapter 6 provides a novel application of HRQAR, where it is to verify selective irradiation of the gut microvasculature in a study of the cause of post-irradiation gastrointestinal syndrome. Chapter 7 will conclude the thesis, and offer suggestions for future work. Two appendices are provided as a quick HRQAR reference to be used when the researcher has some experience. Appendix A gives a concise, step-by-step walkthrough of the procedure, and Appendix B collects all reagent formulae in one list, as well as the manufacturers and part numbers of the particular reagents we used.

---

[1] Kamida A, Obayashi S, Kato I, Ono K, Suzuki M, Nagata K, Sakurai Y, Yura Y. "Effects of Boron Neutron Capture Therapy on Human Oral Squamous Cell Carcinoma in a Nude Mouse Model." *Int J Radiat Biol.* Jan;82(1):21-29, 2006.

[2] Chatterjee, A and Schafer, HJ. "Microdosimetric Structure of Heavy Ion Tracks in Tissue." *Radiation and Environmental Biophysics*, 13, 215-227, 1976.

[3] Coderre JA, Morris GM. "The Radiation Biology of Boron Neutron Capture Therapy." *Radiat Res.* Jan;151(1):1-18, 1999.
[4] Kiger III, WS. Developments in Micro- and Macro-Dosimetry of Boron Neutron Capture Therapy. MIT, PhD Thesis, 2000.

Chapter 2
High Resolution Quantitative Auto-Radiography

2.1 Introduction

The purpose of this chapter is to provide step-by-step instruction on how to perform HRQAR, with comments on how we have modified the technique from the (previously) most recent comprehensive reference on HRQAR.[1] A concise, "cookbook" formulation is included in Appendix A for convenience, and a list of formulae appears in Appendix B.

Before launching into the technique, a brief comment should be made on safety: many dangerous chemicals are used in the preparation of autoradiograms. Be familiar with the material safety data sheets of all reagents, and have a fume hood and the appropriate storage cabinets available. In particular, we found that attaching a bottle-top dispenser, VWR part # 40000-068, to the dichloromethane jug was handy, as that chemical is particularly hazardous, and dispensing it from a large, four liter jug was a bit clumsy.

2.2 Outline

Traditional heavy charged particle autoradiography has been in practice for decades, and one of its chief appeals is its simplicity. Polycarbonate films such as LR-115 and CR-39, when exposed to heavy charged particles, sustain localized damage in the form of broken polymer chains. The film is then etched, and the damaged portion etches faster than the bulk rate, allowing visualization with a light microscope. The

difficulty in applying autoradiography to the study of boron-10 distribution in tissue is the need to correlate visualized tracks with the intracellular location of a capture reaction. Tissue dissolves readily in the caustic etchants. Complicating matters is that the tissue must be stained, in order to identify any cellular structures. Boron-10 is water soluble and will migrate if the tissue is moistened with stain.

HRQAR is a novel but intricate way to circumvent these issues. By the time one is ready to etch the polycarbonate track detector, the stained tissue is safely covered by a 0.7 μm layer of etchant-resistant polymer. The steps to achieve this, presented in the following sections of this chapter, require patience, attention to detail and practice, with particular emphasis on patience. Kiger[1] drew an outline of the HRQAR steps, which is reproduced here for the reader's convenience.

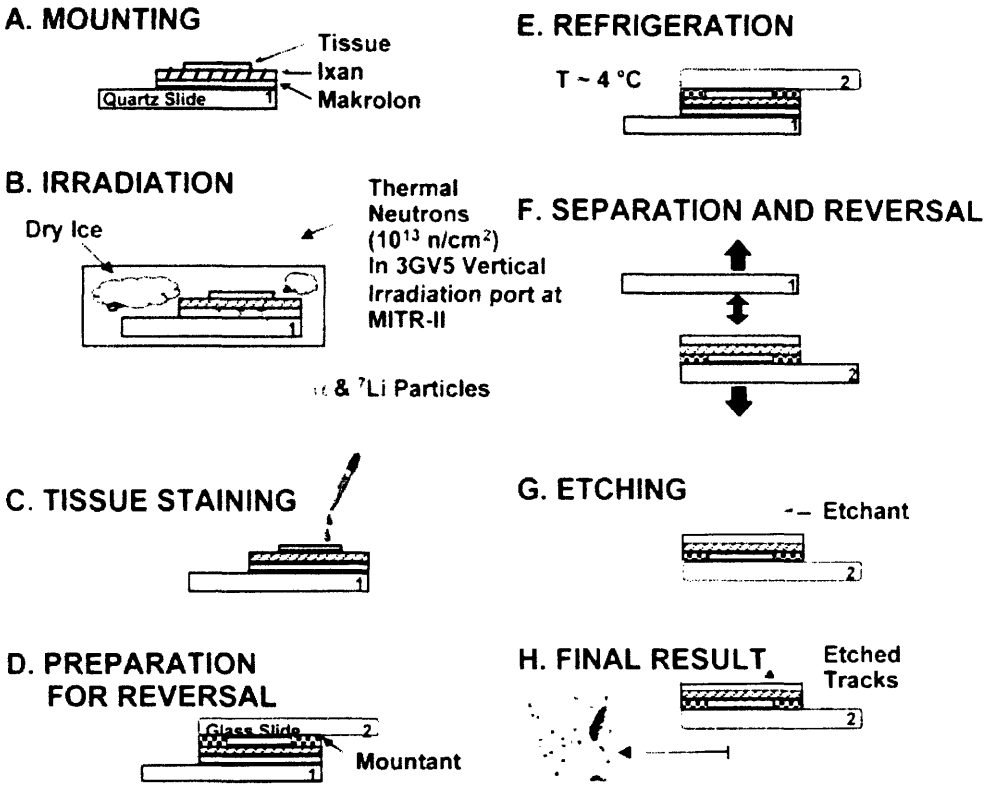

(Figure 2.1 Steps of HRQAR)

To give a better idea of the time frames involved, and the state of the sample at each step, the table below has been prepared.

Step	Time Spent in Step	Temperature of Sample °C
Sample *in vivo*	Varies	Body Temperature
Frozen in liquid nitrogen	~10 seconds	-210
Stored in freezer	Varies	-80
Cryosectioning; A	~1 hour	~ -20
B (tracks produced)	~ 40 minutes	-40 – -20
Post-irradiation decay	1-2 days	-80
C	30 minutes	Room
D	15 minutes	Room
E	2-3 Days	4
F	10 minutes	Room
G	20-40 minutes	Room
H	~1 hour	Room

2.3 Makrolon Coating

The initial slides used in HRQAR should always be made of quartz; otherwise, the boron content of glass will produce false tracks in the makrolon. We used Alfa Aesar

slides (part# 42297) with good results. The slide used in the reversal process should be glass, as it is never irradiated and quartz slides are relatively expensive (~$20 per slide). Before any coatings are applied, the quartz slide must be thoroughly washed with Alconox® (VWR part# 21835-032). This step is critical in ensuring a clean removal of the polymer layers from the quartz slide during reversal. Our experience shows that poor cleaning, or using a different detergent, dramatically affects the reversal success rate, though the reason for why this particular brand is necessary is not yet clear. We have observed that the detergent leaves behind a film, which is difficult to rinse off, and we hypothesize that this film may play a role.

The makrolon solution is prepared in the following manner:

Makrolon Solution

1. Makrolon resin 42.4 g
2. Dichloromethane 487.6 g

Dissolve the resin in dichloromethane, lightly stirring until fully dissolved, leaving a clear, colorless liquid. How long this takes ranges from about 6 hours to several days, depending on how much clumping occurs and the speed of the magnetic stir bar (though as will be explained shortly, one should not be tempted to set a very high rotation speed for the stir bar in order to speed up the process).

Special care needs to be taken with the preparation and handling of this solution, as artifact formation in the final HRQAR image will occur if there is any improper handling. Makrolon is light sensitive. Wrap the storage jar in aluminum foil, and remove it only when necessary. Makrolon has a shelf life of about 1-2 months, depending on how frequently it is used and exposed to air and light. The solution should be frequently weighed, as changes in mass indicate dichloromethane

evaporation, which will change the polymer's characteristics. One pernicious problem we encountered was the formation of air bubbles in the final makrolon polymer layer. This issue resolved after we made two changes to our procedure. First, we stirred the solution very lightly, or not at all, to eliminate any possible introduction of air into the solution. Makrolon is fairly viscous, and any air introduced will not readily bubble out. Second, we changed the storage jar. At first, we stored the makrolon solution in a bottleneck jar, and when solution was needed, it was poured into a beaker. Afterwards, the leftover amount was poured back into the storage jar. Frequent pouring further introduced air bubbles into the solution. We switched from the bottleneck jar to a Qorpak® wide-mouth jar (part# 7985), pre-cleaned with Alconox®. The jar's mouth is wide enough to accommodate the dipping apparatus, and the cap is lined with Teflon, which has been experimentally proven to resist long-term degradation by dichloromethane. By minimizing stirring, and using our particular Qorpak® jars, we eliminated the bubble formation problem.

Figures 2.2 and 2.3 show the makrolon dipping mechanism devised by Kiger[1]. The Qorpak® jar rests on an aluminum plate, glued onto a Styrofoam float. Water is pumped into the reservoir, lifting the float and jar, so as to submerge the hanging slides in the makrolon solution. Water is then siphoned out of the reservoir, leaving a thin film of solution behind. The dichloromethane quickly evaporates, leaving behind a polymer coating.

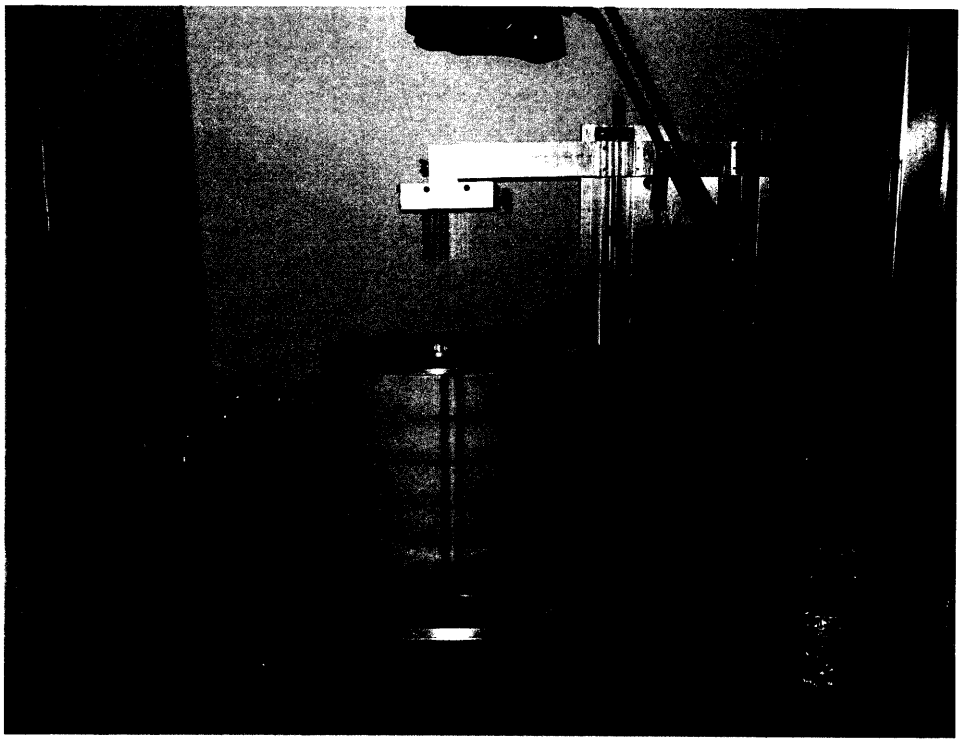

(Figure 2.2 The makrolon dipping mechanism. Foil-wrapped Qorpak jars in the bottom right of the picture fit snugly in the circular opening of the float.)

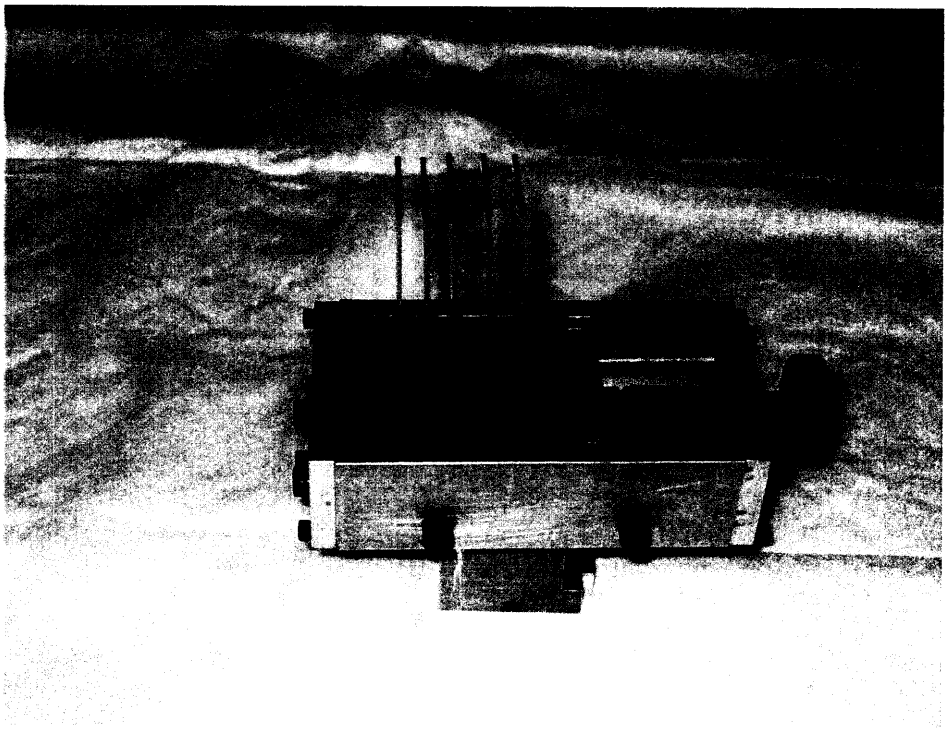

(Figure 2.3 A close up of the slide holder with rubber spacers.)

It has been experimentally determined that a siphon rate of 4 cm/min yields a film thickness of 0.8 μm.[1] The siphon rate should be checked before dipping. Although the rate will vary based on the amount of water remaining in the tank, it remains almost constant over the several centimeters of quartz slide to be coated. The thickness of the film can be verified by observing the interference colors produced by fluorescent lighting.

Makrolon film thickness	Color observed at 45°
6686 Å	Blue
7365 Å	Blue/purple
7923 Å	Purple/red
8100 Å	Purple/red
8702 Å	Green

[2]

Blue/purple to purple/red are the target refraction colors. Once applied to the quartz slides, great care needs to be taken to avoid any contact with the delicate film; any exposure to dust should be minimized by using a clean slide box. Allow the slide about 24 hours to dry.

2.4 Ixan Coating

Once the makrolon coating is applied and dry, two layers of ixan should be coated on. The recipe for the ixan solution follows:

Ixan Solution

1. Ixan Resin 12.6 g
2. n-Butylacetate 30.0 g
3. Trichloroethylene 57.9 g
4. Cyclohexanone 0.8 g
5. Dibutylphthalate 1.6 g

First, mix the ixan resin in the n-butylacetate, stirring with a stir bar until fully dissolved (at least 6 hours). The solution should have a dark yellow color at this point. Add the trichloroethylene, and stir for 24 hours. Filter this solution using a Millipore polypropylene prefilter (type AN12, catalog # AN1204700); we found that drawing a vacuum sped up this process greatly. Finally, add the cyclohexanone and dibutylphthalate, and stir for another 24 hours. If the solution is stored in a clean, sealed, aluminum foil-wrapped container, the shelf life is unlimited.[3]

Application of an ixan layer varies greatly from the procedure for makrolon. Rather than dipping the slide into a reservoir of solution, a droplet of ixan is deposited into a water bath where, due to its hydrophobicity, it will spread out radially on the surface of the water. The various solvents in the solution evaporate, leaving behind a thin ixan film.

The water bath can be drawn from tap water, so long as it is dust free. A disposable pipette is used to deposit the ixan droplet. The tip should be close to, but not touching, the water. If the drop falls from too great a height, it will sink below the surface, and become unusable. Similar to the makrolon, color interference patterns under a fluorescent lamp can be used to assess the thickness, and thus the viability, of a given polymer casting. Figure 2.4 shows a good result of a casting, figure 2.5 a poor one. The bright yellow color in 2.4 indicates a correct thickness,

and the suitable region is large enough to accommodate a microscope slide. Increasing the temperature of the water has been observed to increase the evaporation rate, creating thicker films, though much thicker than yellow films are not required. We find 40 - 45 °C to be a good compromise. The correlation between color and thickness was previously measured:

Ixan film thickness	Color observed at 45°
1594 Å	Gold
2082 Å	Violet
2251 Å	Blue
2315 Å	Blue
2438 Å	Blue/green
2628 Å	Green
2745 Å	Yellow
3057 Å	Yellow/red
3177 Å	Red
3368 Å	Red/violet
3487 Å	Purple/red

[2]

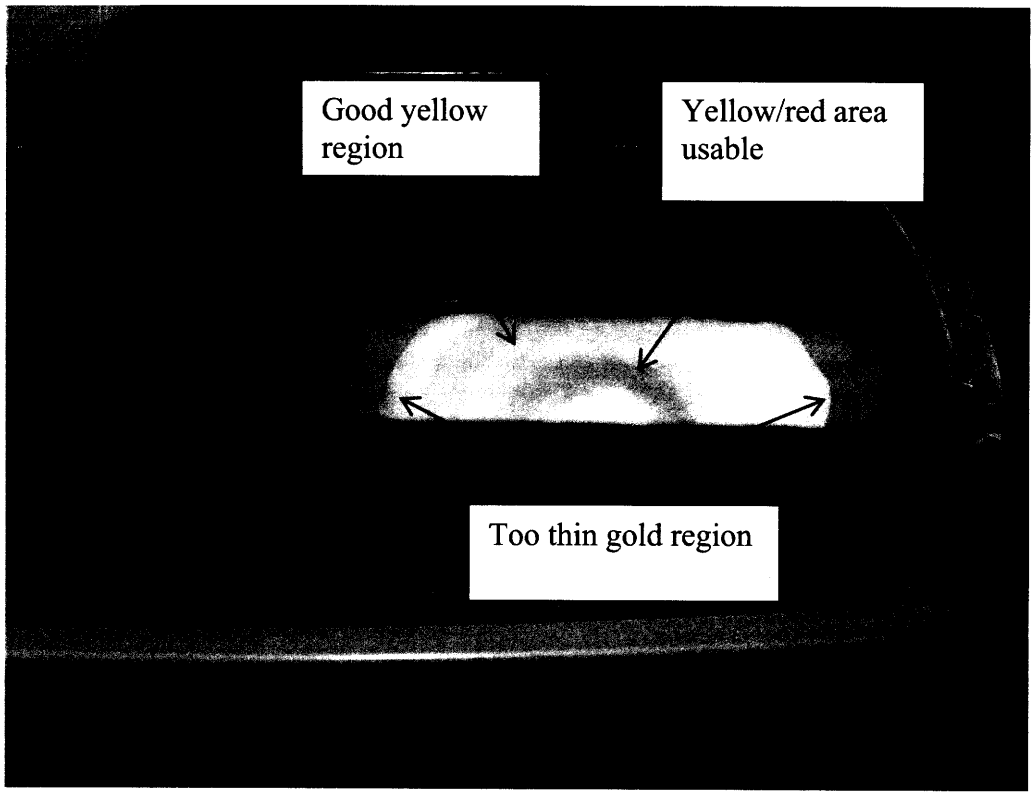

(Figure 2.4 A good ixan casting)

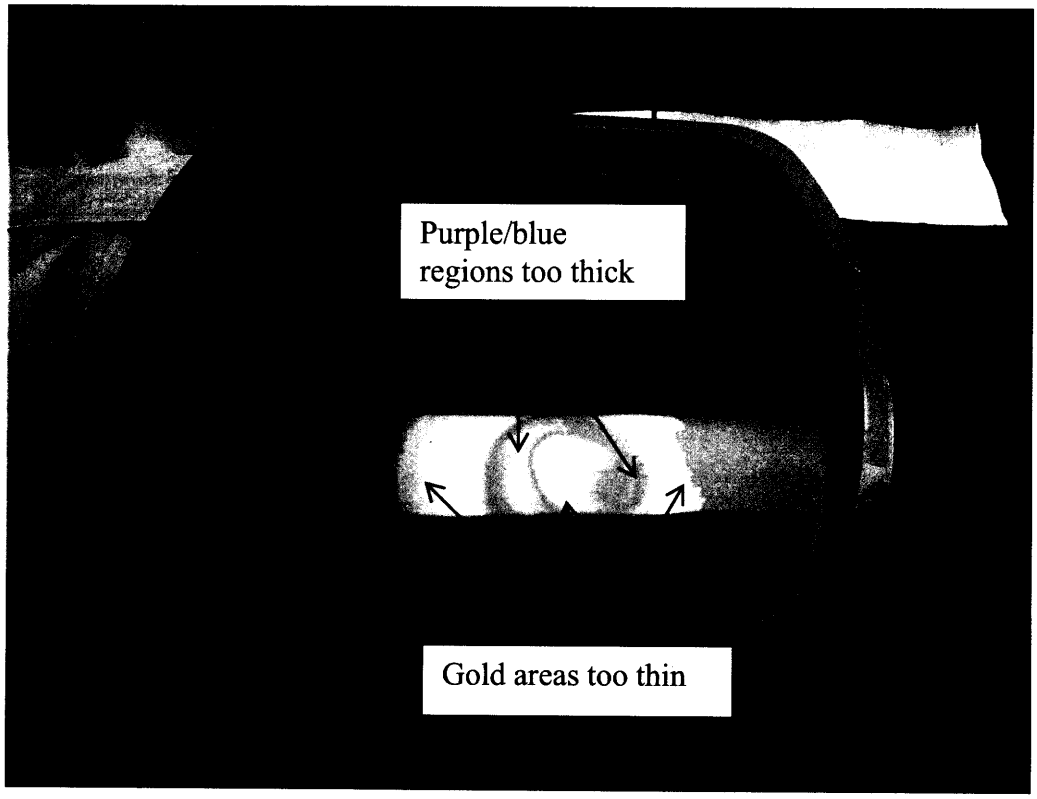

(Figure 2.5 Poor ixan casting)

When a film of suitable thickness – over a contiguous area great enough to coat the makrolon layer on the quartz slide – has been cast, the slide may then be coated. First, grasp the slide by the handle, and lower it vertically into the water bath, so as to minimize accumulation of any debris from the water surface. Once fully submerged, make the slide horizontal, and bring it under the suitable portion of the ixan film. Then, with the far end of the slide leading, bring the slide straight up, out of the water. The good ixan part should now be covering the makrolon portion of the slide. The ixan is sticky, and will adhere well to the slide. Any leftover ixan should be wrapped up on the back of the quartz by rocking the slide back and forth. After allowing the water to dry (~ 6 hours), add a second ixan coating.

2.5 Lamination

Once the second ixan coating is dry, all the polymer layers need to be laminated together. Lamination ensures that, upon reversal, every layer is transferred to the new slide.

Lamination is performed one slide at a time, using dichloromethane. We used a Petri dish with teflon spacers (which are resistant to being dissolved in the solvent) one centimeter in diameter. Efforts to make a larger container, in order to accommodate multiple slide laminations, all resulted in failed reversals. We believe that the small volume of a Petri dish allows for a fast, uniform lamination by the dichloromethane fumes.

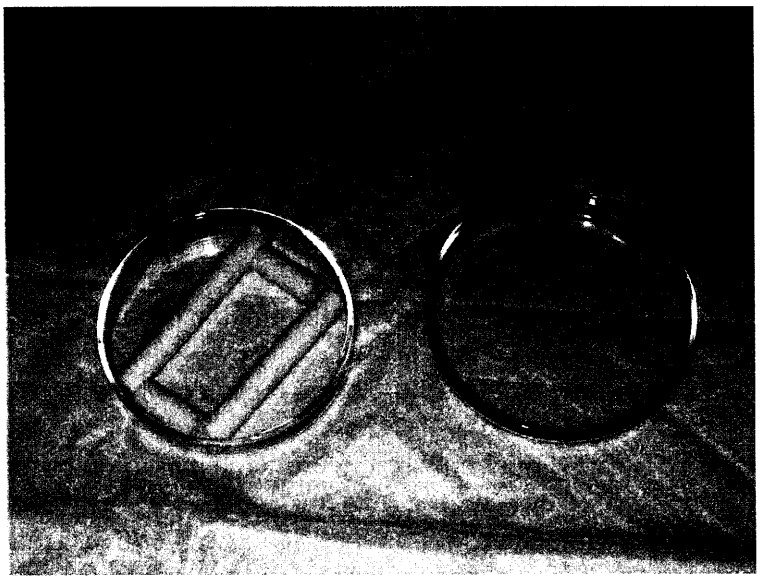

(Figure 2.6 Petri dish with teflon spacers)

After filling the dish with enough dichloromethane to half-submerge the teflon (the vapors, not the liquid, do the laminating), a slide is placed face-down on the spacers, and the dish is covered. After 40 seconds, remove the slide. Slides that have been over-laminated will appear foggy. Once laminated, place the slides in a -80 °C freezer to pre-chill them for the next step.

2.6 Cryogenic Sectioning

Every effort should be made to keep the tissue sample as cold as possible until after the irradiation. Freezing the tissue helps prevent diffusion of the boron before tracks are created, which would destroy any claims to sub-cellular accuracy for HRQAR. We start by freezing tissue in liquid nitrogen, then storing it in a -80 °C freezer; slowly chilling tissue has been shown to exacerbate cell damage caused by

ice crystal formation.[4] Sectioning is performed on a cryo-microtome, using Tissue-Tek optimal cutting compound, at about -20°C, generally in 4 μm sections. Thinner slices, while preferable, can often be difficult to obtain, and larger slices worsen the spatial resolution. After transferring the section to a coated quartz slide, the section is briefly "melted" onto the slide to fix it. This is achieved by lightly pressing the back of the slide to a warm surface, such as one's gloved hand, for several seconds. The slide is then immediately transferred back into the -80 °C freezer. Considerable debate, without resolution, exists regarding the extent of boron redistribution during this brief (< 5 seconds) thaw, and at least one research group feels the need to create special substrates to avoid the necessity of melting tissue samples.[5]

2.7 Thermal Neutron Irradiation

Before 2005, all irradiations were done in the 3GV port of the MIT reactor, as specified in Kiger's thesis. The 3GV port is a vertical thimble in the graphite reflector, accessible from the reactor top, and is surrounded by a water cooled jacket that keeps the temperature of the thimble at ~50 °C. The neutrons are mostly thermal, and fairly uniform. Kiger's original slide holders (figure 2.7) were used. Made of polyethylene with nylon rods, the activation is minimal.

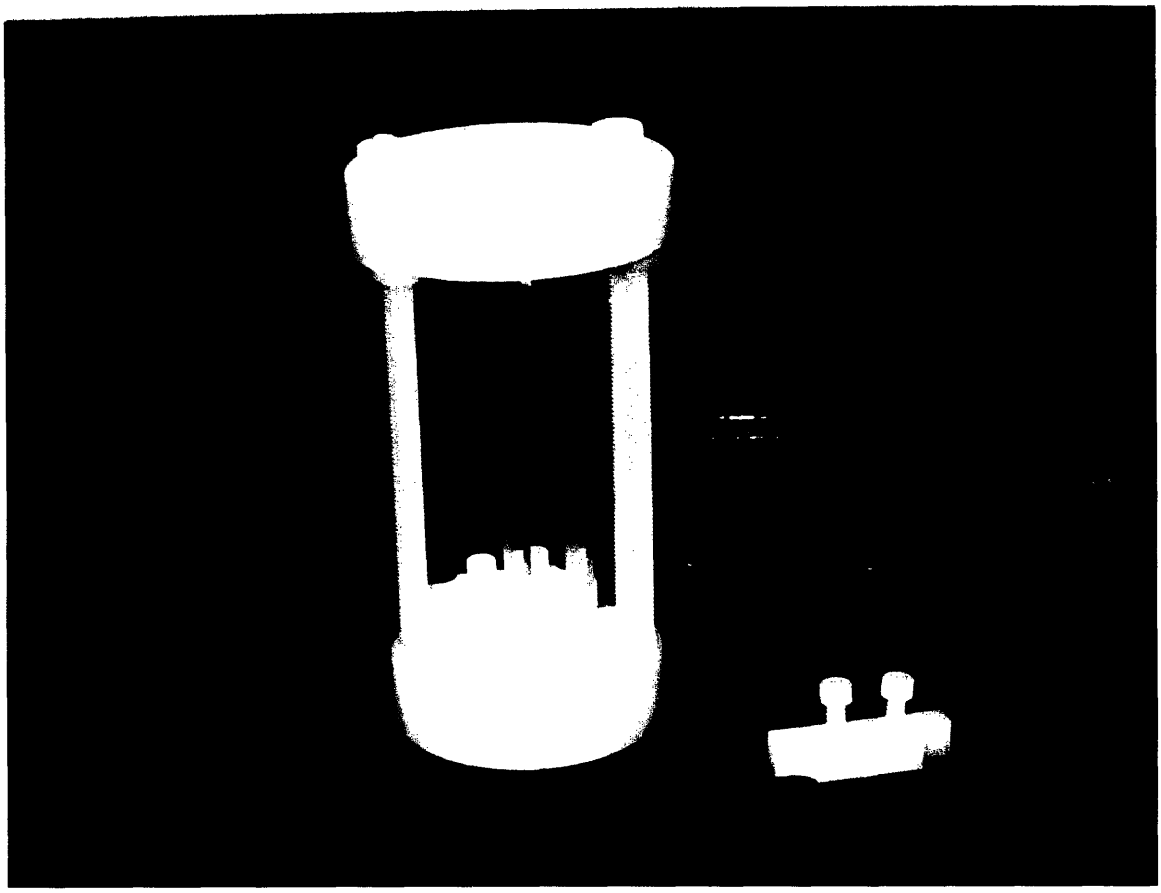

(Figure 2.7 3GV slide carousel with two slides)

The holders are pre-chilled in the -80 °C freezer, loaded with up to 14 slides, then transported to the reactor top in a cooler pack with dry ice. The aluminum tube for the 3GV port is partially filled with dry ice, and then 1-3 holders are placed into the tube. The target fluence will vary depending on the expected boron concentration range in the sample. As a benchmark, we measured a fluence of ~1 x 10^{13} n/cm^2 after a 2 minute irradiation with the reactor power at 30 kW, and this fluence was generally sufficient for most samples, though at times we increased irradiation time to 4 minutes for samples with smaller B10 concentrations. To further ensure uniformity of boron irradiation, we rotated the holders a quarter turn every 30 seconds. After

being removed from the beam, the samples are given a 15 minute decay time, then transferred back to the -80 °C freezer via the dry ice-packed cooler. Let the samples sit for 1-2 days to decay before handling.

Using the 3GV port has several advantages in that a relatively large number of slides (up to 40) can be irradiated at once, and rather quickly. However, the MIT reactor generally operates at 5 MW. Dropping the power to 30 kW, irradiating, then returning back to full power generates so much downtime for the reactor that we were limited to performing irradiations during normally scheduled reactor shutdowns and startups – generally about once or twice a month. We decided that adapting this procedure to our medical thermal neutron beam would be preferable, despite necessitating a longer irradiation time, and limiting the number of slides irradiated at once to 10. The thermal neutron beam can be operated regardless of the reactor power, thus giving us considerable flexibility in running experiments.

The change necessitated a redesign of our slide holder. The M-011 vertical thermal neutron beam port extends from the D_2O reflector/moderator below the core, down to the medical room in the basement of the facility. Between the D_2O tank and the basement lie an H_2O shutter tank, graphite collimator, boral shutter, lead shutter, and a bismuth plug in a bismuth collimator. Four fission counters are placed at 90° intervals on a borated polyethylene plate delimiter below the lead shutter, and monitor beam intensity and symmetry. The thermal beam port is a 12cm diameter aperture in the ceiling of the medical room.[6]

A new slide holder, shown in figure 2.8, was designed for use in the new facility. It is made of polyethylene in order to improve fluence with backscatter, and

accommodates up to 10 slides at once. Slides in the outside row are placed with the tissue-containing portion of the slide facing inward, and the second row's slides will face the opposite direction. The central axis for the neutron beam falls halfway between the two middle slide grooves.

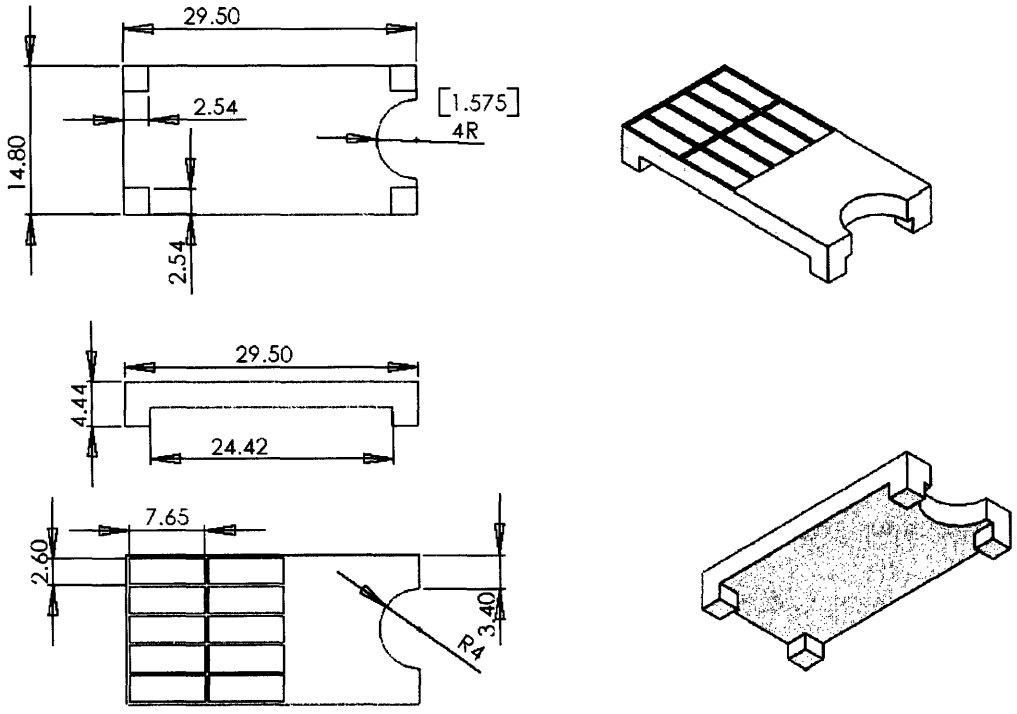

(Figure 2.8 M-011 slide holder; dimensions in centimeters)

The holder is placed in a lithiated polyethylene box, which is secured to the ceiling port by four nylon screws. At the halfway point of the irradiation, the beam is stopped, and the slides are rearranged to insure uniformity in fluence. Slides at the edge are moved to the middle, and vice versa. This shuffling produces fluences consistent to 3.3%; 1 mm setup error and beam counter uncertainties account for 2.2%.

To keep the samples as cold as possible during the irradiation, which can last ~ 40 minutes, the holder is pre-chilled in a -80 °C freezer before use. Dry ice is placed on the holder, as well as directly on the non-coated portions of the slides. During the slide swapping at the halfway point, this dry ice should be replenished. Temperature measurements show that samples start the irradiation at ~ -40 °C, and do not drop below -20 °C by the termination of irradiation.

2.8 Hematoxylin & Eosin Staining

Hematoxylin and eosin staining is used to visualize the structure of the sample: hematoxylin stains nuclei blue, and eosin dyes the cytoplasm pink. Other staining types might be useful as well, though they should be tested first to see if they damage the thin polymers. Our H&E staining differs from general laboratory practice in that the stain is applied via droplets onto a level slide, rather than vertically immersing them in the dyes. The reason for the change stems from the weak bond of the tissue with the polymers – it tends to flush right off. Even in this modified procedure delicacy is require, in order not to lose the tissue.

H&E Staining

1. 70% ethanol: With the slide positioned at an angle (~45°) pour about 10 drops of ethanol above the tissue, letting it moisten the tissue as it runs down.

2. 50% ethanol: With the slide positioned at an angle (~45°) pour about 10 drops of ethanol as above.

3. Distilled water: Pour about 10 drops as above.

4. Harris hematoxylin: Place the slide on a flat surface and place enough drops of hematoxylin so as to completely cover the tissue. The time needed will vary with different tissue types, so some initial experimentation will be necessary, but generally around 16 minutes is sufficient.

5. Tap water: Rinse until the hematoxylin is completely removed.

6. Acid alcohol: Pour 3 to 8 drops as in step 1.

7. Tap water: Pour 10 drops above the tissue to rinse the acid alcohol away.

8. Ammonia water or lithium carbonate: Pour either one (we used lithium carbonate) on the tissue until it turns bright blue.

9. Tap water: Wash several times to ensure complete removal of step 8 component, otherwise the eosin will stain unevenly.

10. Eosin: Place the slide on a flat surface and drop eosin on until the tissue is completely covered. Let soak for 2-3 minutes.

11. 95% ethanol: Several drops until eosin is completely removed.

12. 100% ethanol: Pour 20 drops.

Harris Hematoxylin

1. Harris Hematoxylin 100 ml
2. Glacial Acetic Acid 2-4 ml

Mix and filter before using. Color should be deep purple.

1% Eosin Stock

1. Eosin Y, Water Soluble 1.0 g
2. Distilled Water 20 ml
3. 95% Alcohol 80 ml

Dissolve eosin completely in water, then add alcohol and stir. Color should be an iridescent orange.

Working Eosin Solution

1. 1% Eosin Stock 1 part

2. 80% Alcohol 3 parts
3. Glacial Acetic Acid 0.5 ml/per 100 ml

Just before use, dissolve stock eosin in alcohol, then add acetic acid and stir. Color should be brilliant orange.

Acid Alcohol

1. 70% Alcohol 100 ml
2. Hydrochloric Acid 1 ml

Mix and stir.

Ammonia Water

1. Tap Water 500 ml
2. 28% Ammonium Hydroxide 1 ml

Mix and stir.

Lithium Carbonate

1. Lithium Carbonate 1 g
2. Distilled Water 100 ml

Mix and stir.

2.9 Reversal

Immediately following staining is the reversal step. The intent here is to reverse the order of the various layers on the quartz slide, exposing the information-containing makrolon while placing the tissue beneath the protective ixan. A glycerol/gelatin mountant (Sigma-Aldrich part# GG1) is used to bind the layers to a new, Alconox®-cleaned glass slide. The mountant is warmed in a 55°C water bath, because it is a solid at room temperature, and at warmer temperatures is less viscous,

and less likely to retain bubbles. Place about 5 drops spread out across the makrolon area (see figure 2.9). Depending on the area of the slide to be covered, 5 drops may be insufficient. If in doubt, always add more. Too much mountant creates a small, easily cleaned mess, while too little will ruin the sample. Gently squeeze the glass slide – with its distal end oriented toward the quartz slides handle – about 1 mm past the makrolon line. Firmly squeeze along the region of overlap to expel any bubbles in the mountant. Place the slides in an aluminum foil-lined box, and place in a refrigerator for 2-3 days.

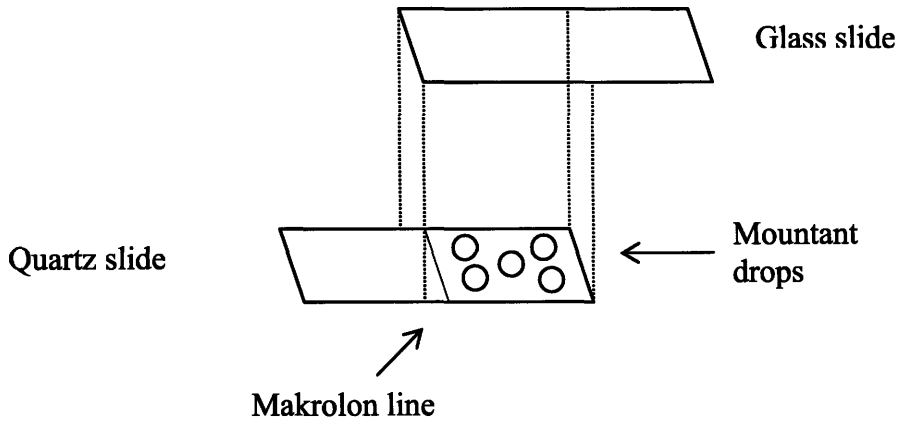

(Figure 2.9 Mounting process)

After allowing the mountant to set in the refrigerator, it is time to separate the two slides. Begin by cleaning off any extra mountant outside the slides, particularly where the two slides meet. Failure to do so may cause the slides to stick together during the next step, which may result in one or both breaking. Once the slides have been carefully cleaned of extra mountant, grab each slide handle, and apply a firm, mutually opposed torque (see figure 2.10). The slides will separate, and all the layers

will transfer to the glass slide. With practice, we achieved a success rate of about 90%.

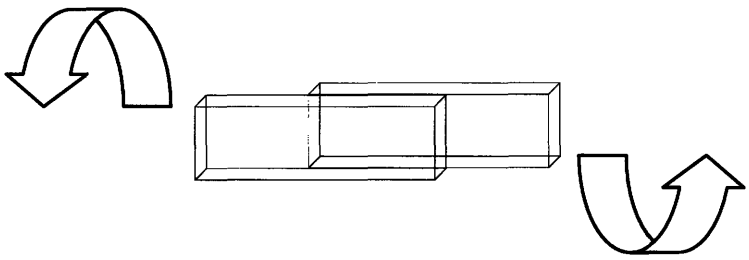

(Figure 2.10 Mutually opposed torques)

2.10 Ixan Painting

As added insurance against etchant leaking through the polymer layers, ixan is painted over regions of makrolon containing no information, that is, the entire film except that directly above tissue, plus a small margin around it (see figure 2.11), in addition to the edge of the slide itself. To paint the slides, we used long-handled, disposable cotton swabs with the tip dipped into our container of ixan. Allow to dry (takes about 15 minutes), then apply a second coating.

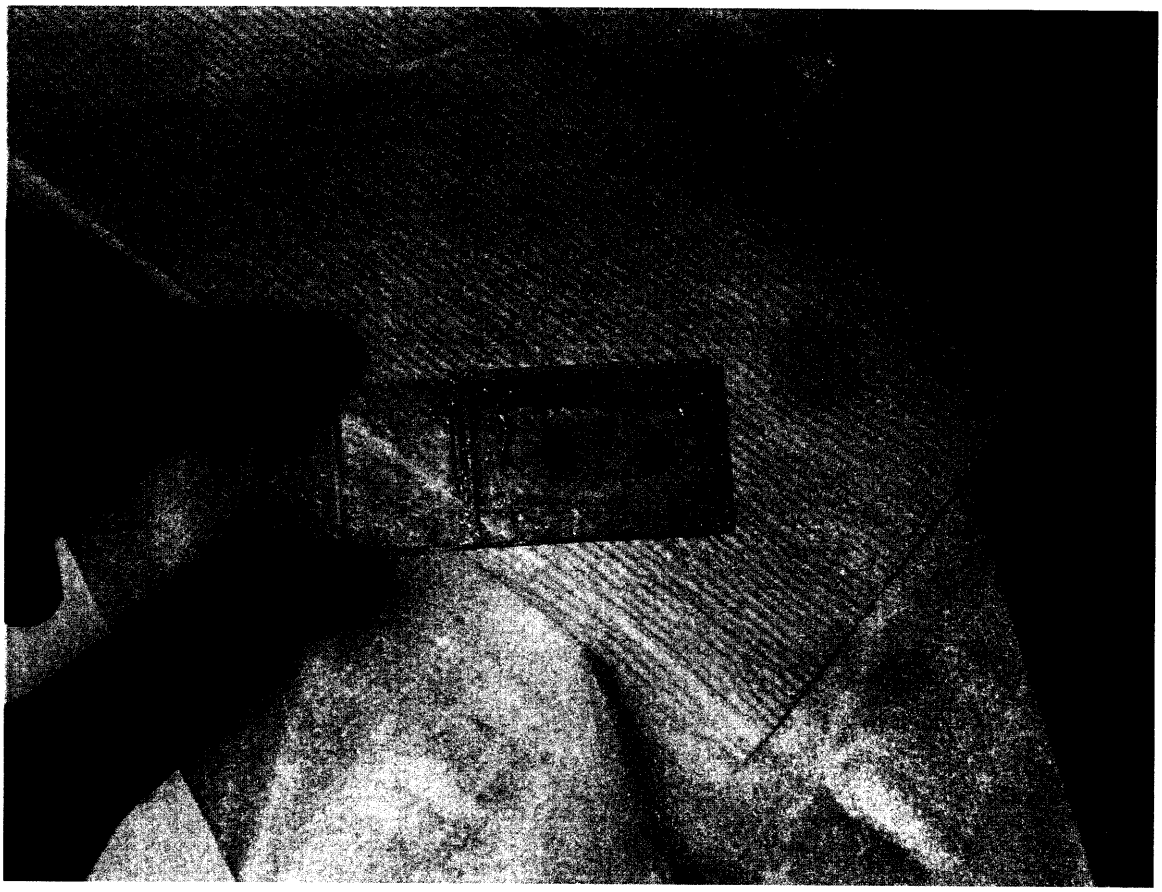

(Figure 2.11 A slide, painted with ixan)

2.11 Etching

The final step in HRQAR is to etch the makrolon layer. Because the passage of a heavy, energetic ion breaks polymer chains, the area of damage will etch faster than the bulk etch rate of makrolon. Thus, "pits" will form, correlating with the location of a ^{10}B capture reaction.

The etchant is made as follows:

KOH Etchant

1. KOH Pellets 9 g
2. Distilled Water 27 g
3. 100% Ethanol 24 g

Mix the pellets in water, cover with parafilm, and stir. Once completely dissolved, add the ethanol, re-cover, and stir. The solution is good for a day or two.

Because the reaction is exothermic, the etchant will be warm. However, we etched at room temperature. So either leave sufficient time for the solution to cool down (several hours), or prepare a water bath at room temperature. Place the slides vertically in the etchant container, and cover with parafilm. Kiger suggests etching for 20-40 minutes, but we found that less than 30 minutes yielded tracks that were superficial, and difficult to image, while etching times of 40 or more minutes tended to ruin the tissue. We therefore recommend an etching time of 30-35 minutes. After removing the etched slides, rinse them in 47% ethanol, and allow the slides to air dry. The next chapter will cover image acquisition and analysis of the slides.

2.12 Conclusion

The steps for preparing slides for HRQAR analysis have been laid out, with a concise version available in appendix A, and a recipe list in appendix B. The method does not radically diverge from Kiger's thesis, but some improvements have been made. By adapting the procedure to make use of the MIT thermal beam, we can conduct irradiations on demand. Also, our experience in resurrecting the technique

has illuminated a list of previously undocumented factors in the success of HRQAR. For example, the particular detergent used to clean the glassware has been identified as critical in successfully reversing the polymer layers. These observations have been transcribed in the appropriate sub-chapters to assist someone starting up the technique from scratch.

---

[1] Kiger III WS. "Developments in Micro- and Macro-Dosimetry of Boron Neutron Capture Therapy," Ph.D. Thesis, Massachusetts Institute of Technology, 2000.
[2] Kirsch JE. "Neutron-Induced Track Etch Autoradiography: Studies in Track Detection and Neutron Capture Therapy," Ph.D. Thesis, Massachusetts Institute of Technology, 1984.
[3] Keyser A, Wijffels C, "The Preparation and Use of Polyvinylidenechloride Protective Films in Autoradiography," *Acta Histochemica*, **Supplement 8**, 359-367, 1968.
[4] Mazur P. "Freezing of Living Cells: Mechanisms and Implications." *Am J Physiol.* 247:C125-C147, 1984.
[5] Chandra S, Smith DR, Morrison GH. "Subcellular Imaging by Dynamic SIMS Ion Microscopy," *Analytical Chemistry*, 72(3): 104A-114A, 2000.
[6] Harling OK, Riley KJ, Binns PJ, Patel H, Coderre JA. "The MIT User Center for Neutron Capture Therapy Research." *Radiation Research* **164**, 221-229, 2005.

Chapter 3
Image Acquisition and Analysis

3.1 Microscopy

After etching, track pits about 1 μm in diameter will be visible. We produced optimal images by using either a 40X or 63X objective, corrected for use without a coverslip. Our equipment was a Leitz Orthoplan microscope with a mounted Olympus Q Color 3 3.3 megapixel CCD camera, attached to a personal computer (see figure 3.1). A Biopoint motorized stage, produced by Ludl Electronic Products (http://www.ludl.com), had been retrofitted to the microscope, allowing X, Y, and Z control via either the attached joystick or the computer software. Motorized stage movements were consistent to about ± 5-6 μm, so "patching" together multiple camera frames into one image has to be done by hand. For image acquisition software, we purchased IP Lab version 3.6.5, from Scanalytics, Inc. Acquired images are saved in .tif multipage format, for the convenience of storing multiple related images in one file. Image analysis is conducted on a lab-written MATLAB code, initially developed by Kiger[1], and explored in detail in Chapter 3.2. The MATLAB microdosimetry code is covered in chapter 4.

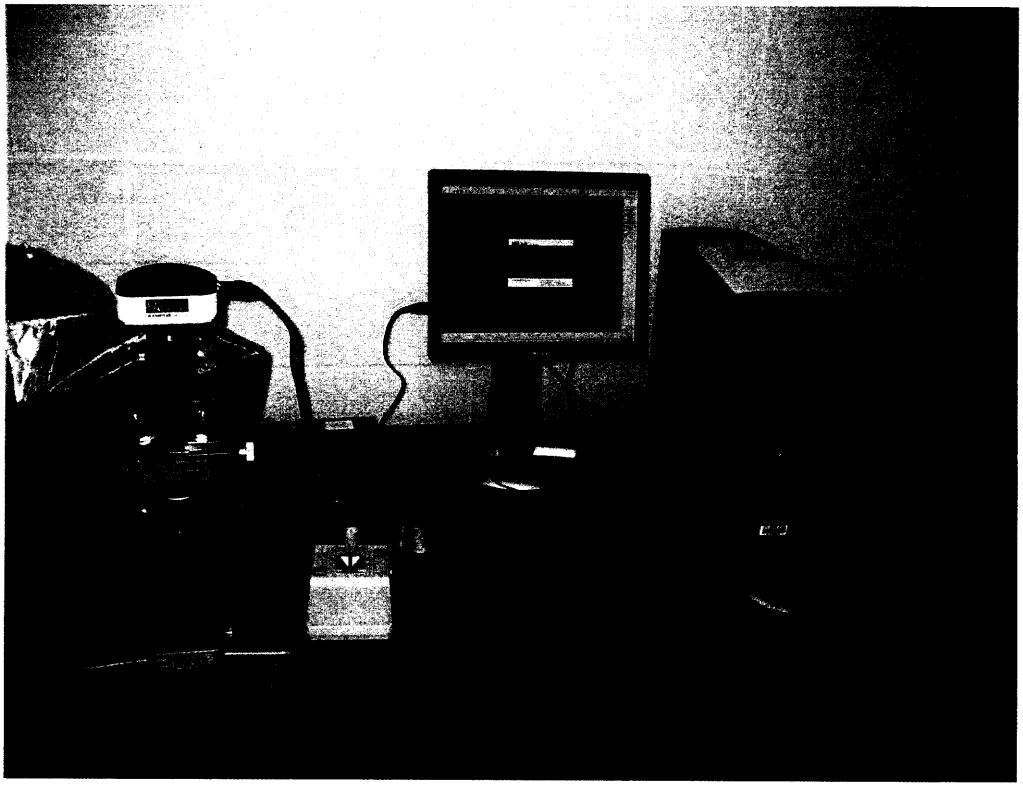

(Figure 3.1 The microscope/computer set-up)

When a suitable section of tissue has been located, three different images of the same section – obtained by varying the focal plane only – are required for processing. One image should focus on the histological features, which will be necessary in delineating appropriate target structures. And the other two images will focus on the tracks themselves: they will appear as black dots in one plane, and as small haloes after adjusting the plane ~ 0.5 μm (see figures 3.2, 3.3 below).

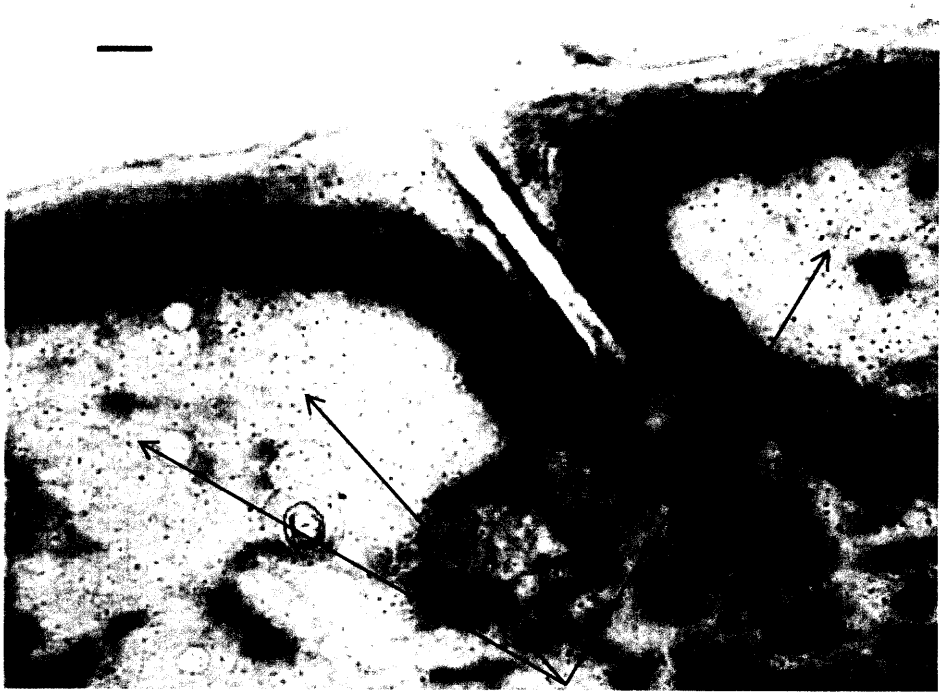

(Figure 3.2 Tracks as black dots. Tissue is rat skin, with a hair follicle. Bar is 10 μm)

(Figure 3.3 Tracks as haloes. Note that besides the tracks, this image is nearly identical to figure 3.2. This allows digital subtraction to ferret out the tracks from background.)

3.2 Track Analysis Software

The Track Analysis program starts by calling the m file trackanalysis.m from the MATLAB command window. After the initial loading screen clears, the gui will appear in the upper right corner of the screen (figure 3.4), with 8 different toggles: image, view, list, method, threshold, object select, morph ops, and count. The image, view, and list controls are on by default.

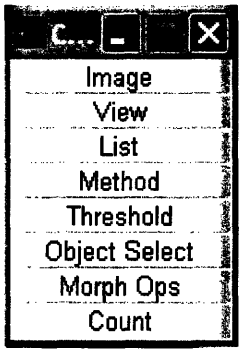

(Figure 3.4 Main control panel)

The image control panel (figure 3.5) controls all external file operations. It is used to open, close, save, and duplicate images. Any image format readable by MATLAB may be used, and if a multipage .tif file is opened, a pull down menu is available to select the page number. Saved images will be single page .tif files.

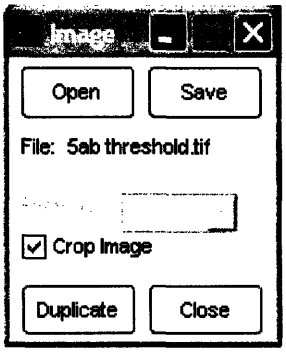

(Figure 3.5 Image control panel)

Options available in the view control panel (figure 3.6) alter how an image is displayed, but do not change the actual image data. Color images may be viewed in full color, grayscale, or as any combination of red, green, and blue. Single component images (grayscale, one of the RGB colors) can have a colormap applied using the box in the bottom right corner. *Expand Histogram* rescales the intensity of the image to occupy the full color space. Equalizing histograms is also possible, but the two checkboxes below are not implemented. In the bottom left corner, one may change the size of the displayed image, and one may select that scale as default for the other images.

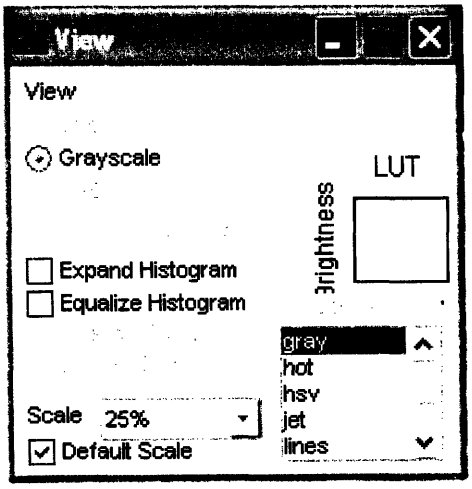

(Figure 3.6 View control panel)

The list control panel lists and allows control over opened images. Image names are in black if displayed and gray if hidden. Right click on the filename will toggle the image between these two states. The currently selected image is highlighted in yellow. The red check box designates a binary image (eg, the tracks only) as a threshold image, and the blue check boxes allow one to overlay the threshold onto other images, for verification purposes.

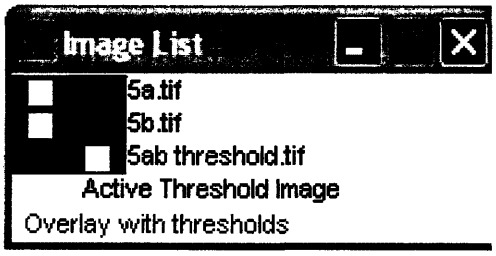

(Figure 3.7 Image List control panel)

The method control panel (figure 3.8) provides the primary means for discriminating tracks from background artifacts. The top pull-down menu allows selection of an image operation, and the two menus below allow the user to select the two images to undergo a digital operation. Subtraction and Division with Limits (same as Division, but saturated pixels are eliminated) are the only operations used in practice, and we have noted that Division with Limits sometimes yields images of smaller size than the originals; we find subtraction to be the most generally useful operator.

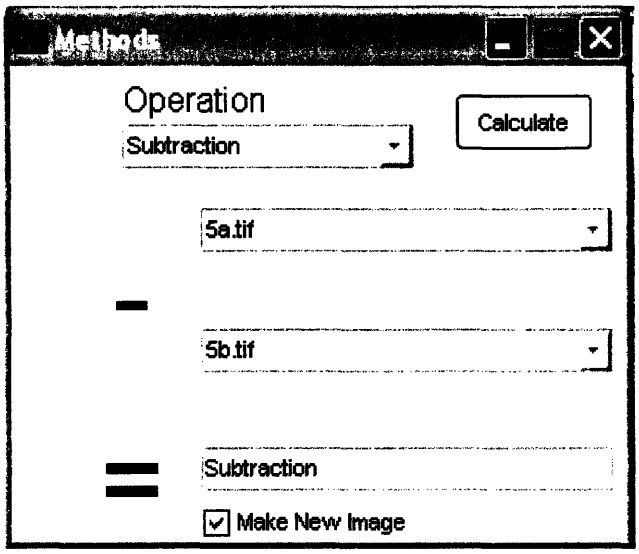

(Figure 3.8 Method control panel)

Image subtraction works well as a first-pass filter, because many artifacts are out of phase with the tracks. The change in focal plane, going from tracks visible as dots to tracks visible as haloes, is relatively small. A speck of dust, which is much larger than a track, would look nearly identical in the two images, and would be subtracted out.

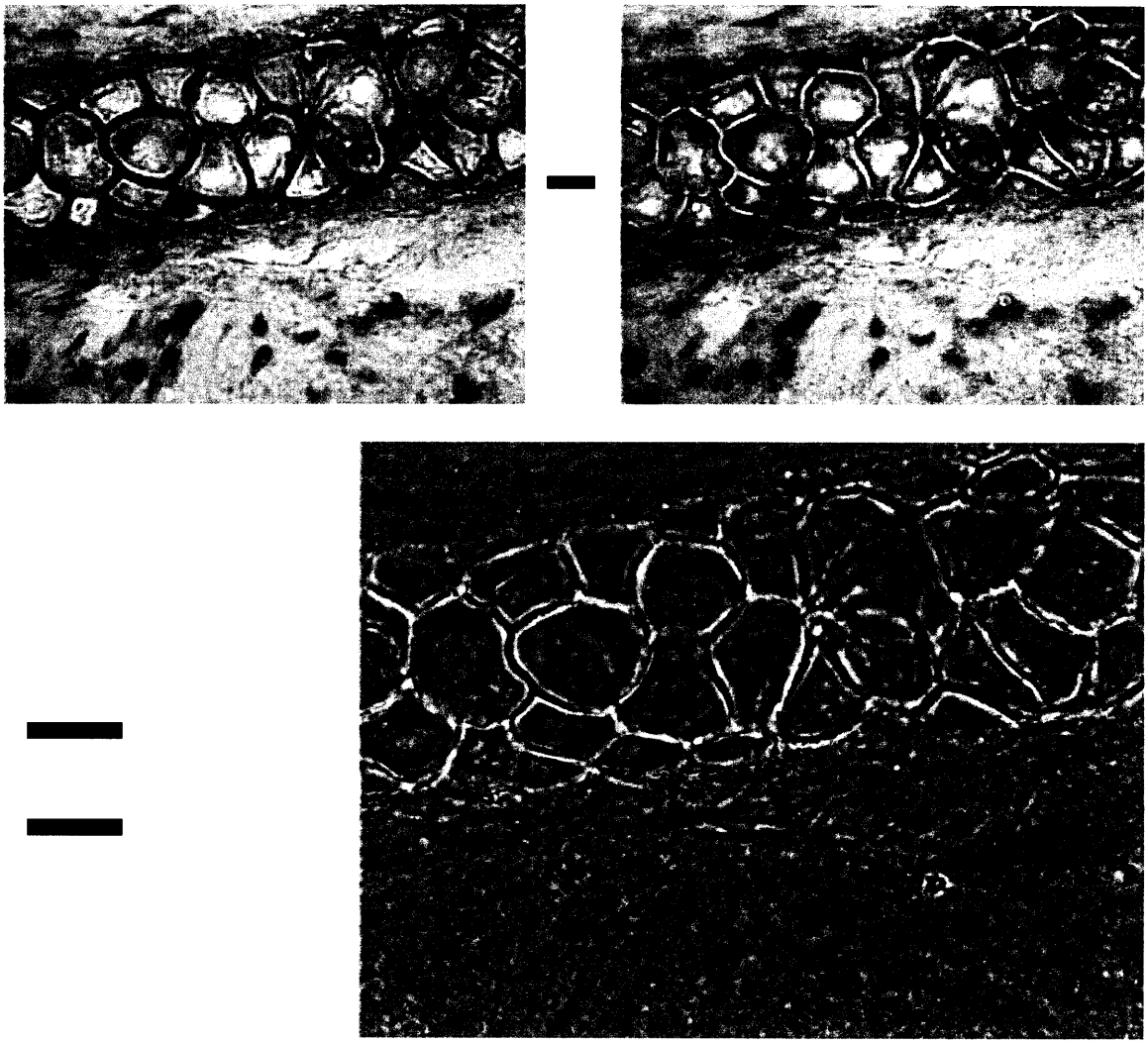

(Figure 3.9 Image subtraction)

The threshold control panel (figure 3.10) provides the next step in track discrimination. Although the tracks undergo the largest change – going from black dots to white haloes – the background is not completely unchanged, as observed in figure 3.9. This control panel allows thresholding in three possible color spaces: RGB (pictured), HSV (hue, saturation, and value), and grayscale (easiest to use, as there is only one slider). After selecting the image to be thresholded from the top pulldown menu, and selecting a color space, the threshold value are set by manually typing numerical values

in, or adjusting the sliders with a mouse. Dragging either end of the bar allows resizing, and dragging the middle will move the bar, while preserving its length.

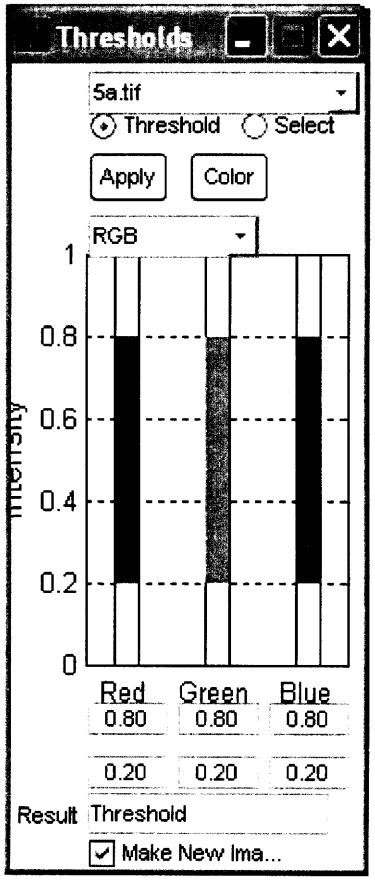

(Figure 3.10 Threshold control panel)

Typing an entry in the *Result* box gives the threshold image a name. Clicking *Apply* will create the new figure, while clicking *Color* will set the highlight color for overlaying a threshold image onto another image. The image produced will be white on a black background.

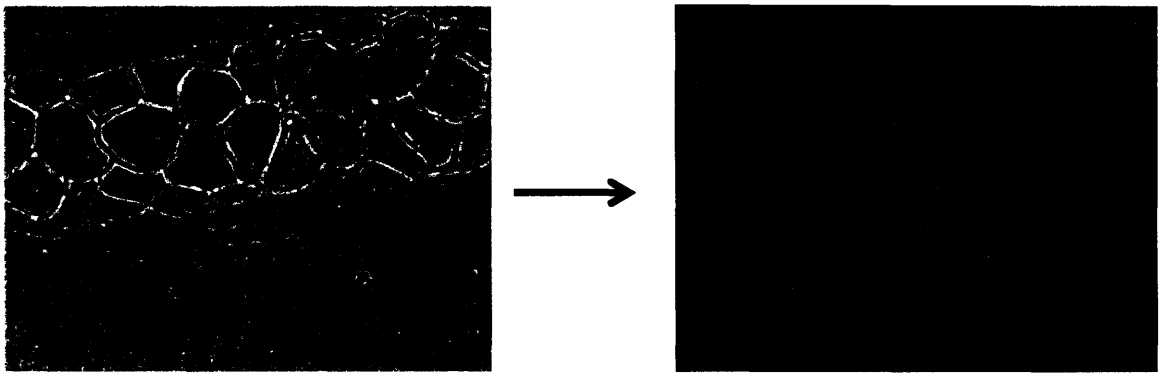

(Figure 3.11 Thresholding)

The object select control panel (figure 3.12) allows further filtering of noise from the threshold image, before manual deletion of such is required. Several filtering bases may be used: area of object, eccentricity, equivalent diameter, and major and minor axis lengths of a best fitted ellipse. In practice, we found the area in pixels to be a quick, intuitive parameter to use. Images less than 4 pixels in size, or greater than 150, are most likely noise, not tracks. To begin, select an image from the pull-down menu on top. The three buttons near the top of the panel create new images: *Select* makes a new images based on user-inputted min and max values in the edit boxes, *Color* produces a greyscale image of the objects, color coded to the select measure, and *Centroid* creates an image only of the centroids of the objects. The *Select* button is the only operation necessary for image analysis. *Histogram* and *EDF* (empirical distribution function) will show analysis of the particular filter basis selected.

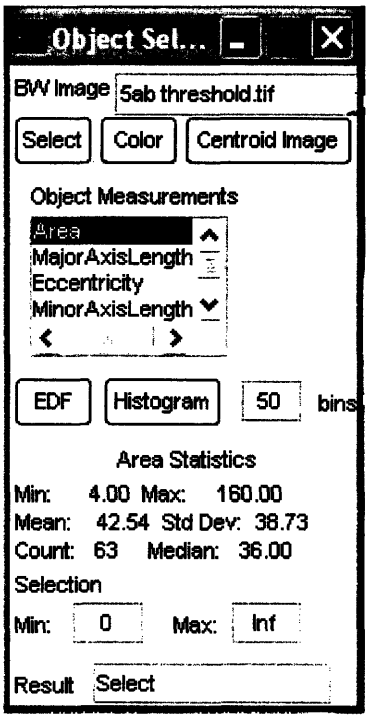

(Figure 3.12 Object Select control panel)

Morphological operations (figure 3.13) is the final step in preparing an image for track counting. It contains one useful function, and seven essentially useless ones. *Erode, dilate, thin, thicken, open, close,* or *shrink* have no known application in HRQAR image analysis. *Erase*, however, can be used to eliminate any artifacts leftover after threshold and object select operations. Click *erase*, drag a box around the object(s) to be eliminated, and click *erase* again.

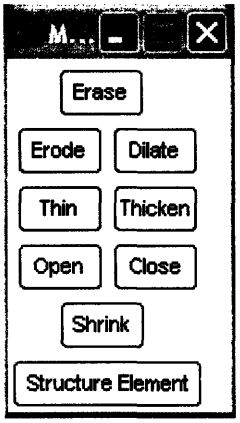

(Figure 3.13 Morphological Operations control panel)

Once an image has been properly pared down to a black background, with white dots representing tracks, some preliminary quantification is possible. To do so, open the count tracks control panel (figure 3.14). This panel calculates the track density in specified regions of interest, and correlates them with previously measured standard samples to determine the ^{10}B concentrations.

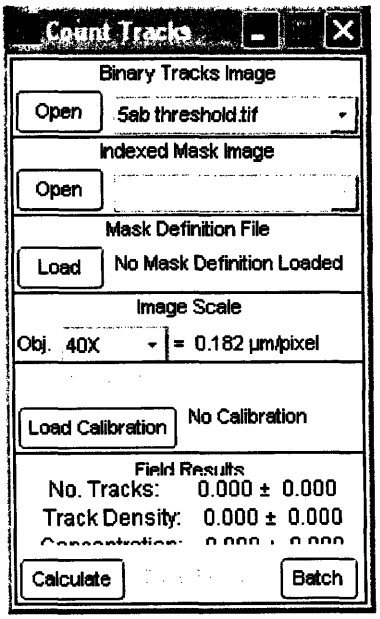

(Figure 3.14 Count Tracks control panel)

The first pull-down menu allows the user to select the binary image to be counted. The second allows the user to define regions of interests, by way of a mask image. Mask images are color-coded maps that outline histological areas of particular interest; cell nuclei are a typical target. Mask images are color-indexed .tif files, 8-bit, and are given the .seg extension to denote a segmented image file. We used Adobe Photoshop in the creation of .seg files. If no file is indicated, the track density of the entire image will be calculated. A mask definition file may be included to label the different areas delineatedin the .seg file, though are not required. The image scale tells the software the actual length represented by a pixel in the image, allowing calculation of tracks per unit area. The exact ratio will depend on the user's equipment. Finally, a calibration curve can be loaded. Calibration data (acquisition of which is discussed in the next section) is stored in MATLAB binary data format, correlates track density with boron concentration, and is ideally created anew for each experiment. This is, however, unnecessary, as the data can be scaled linearly by the difference in neutron fluence between experiments. This highlights another advantage to switching our irradiations to the thermal beam facility from the vertical thimble port: the tight, reproducible control this offers us over the neutron fluence, making for a small difference between irradiations. If no calibrations curve is loaded, only track densities are calculated.

Once all of the appropriate menus are set, calculations of track density and boron concentration (if applicable) start by clicking *Calculate*. Average quantities for the entire field are displayed at the bottom of the control panel; to access values for the various regions of interest, click *Save Results* to save the information to a text file. *Batch* will

bring up a dialog box to select a binary track image. After doing so, all other track images in the active directory are analyzed as well.

3.3 Standards Preparation

In order to calibrate the MATLAB file expressing the linear relationship between track density and boron concentration, samples with a known, homogenous boron concentration need to be used as standards. This is accomplished by soaking tissue in an aqueous solution containing deionized water, 20% sucrose by mass, and NIST traceable boric acid 1000±10 mg B/ml. The tissue used should ideally be the same tissue analyzed in the experiment, though this is not always practical. We used whole mouse brains, and Kiger suggests buying chicken liver from the grocery store as a convenient alternative.[1] The sugar is added to help extract water from the cells, allowing less damage to occur during freezing. Add boric acid to achieve the desired ^{10}B concentration; recall that boron-10 constitutes 18.34% of naturally occurring boron. Standard concentrations should bound the concentrations expected in the sample; generally, we used concentrations of 5, 10, 20, 50, and 100 ppm. Verify the ^{10}B concentration in your standards using a technique such as prompt gamma neutron activation analysis. Submerge the tissue in the solution, and store at 4°C for seven days. Patel notes that tissue will generally float at first, then sink as the solution displaces air from the sample.[2] After the week, freeze the tissue, and store in a -80 °C freezer.

---

[1] Kiger III WS, "Developments in Micro- and Macro-Dosimetry of Boron Neutron Capture Therapy," Ph.D. Thesis, Massachusetts Institute of Technology, 2000.
[2] Patel H. Personal communication, 2003.

Chapter 4
Microdosimetry Software

4.1 Introduction

The microdosimetry software used is a two dimensional Monte Carlo simulation of charged particle transport, originally written by Kiger using MATLAB[1], and updated recently for use in newer version of MATLAB and Windows. The software, BONCRES (**BO**ron **N**eutron **C**apt**uRE** **S**imulation), uses surrogate 2-D modeling, using the principle of stereology.[2] In essence, the histological section – a random plane through tissue, containing randomly oriented cross sections of cells – is equivalent to sampling a representative three-dimensional cell with a number or randomly oriented planes.

This chapter will explain the user end of the software, as well as how the microdosimetry and statistics are calculated. We will then give the results of verification test run to verify the accuracy of the software.

4.2 Software Inputs

Boncres takes up two four different input files: a segmented image outlining the geometry of the problem and a text file detailing the different simulation parameters are required, and a histological image and a tracks image are optional.

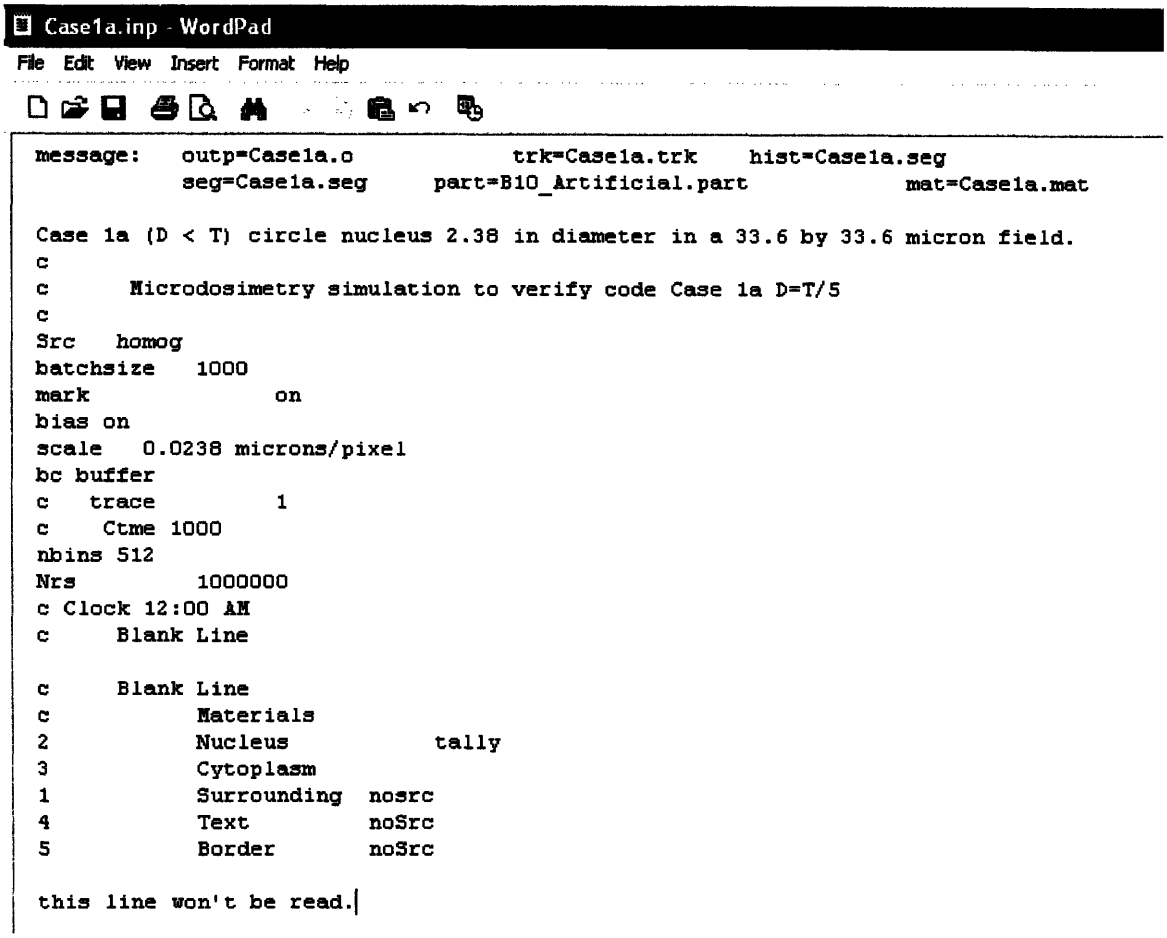

(Figure 4.1 Sample input deck)

Pictured above in figure 4.1 is a sample text input deck. Everything following a "c" is a comment. The first two lines, called the message block, specify the locations of 5 different input/output files. outp specifies the filename to save the result of the simulation. trk indicates the name of the optional track image file. hist locates the optional histological image file. seg specifies the segmented image file that details the simulation's geometry. And part indicates which file contains the charges particle data. A blank line is necessary to indicate the end of the message block. If the files are not all in the same directory, an absolute path is required.

After the blank line one types in a title. There are two options for "src," the source definition: "homog" for homogenous or "tracks" for a distribution supplied by TrackAnalysis. "Batchsize" sets the reaction batch size. "Mark" and "trace" are optional cards, and will draw the source locations and charge particle paths, respectively, on the histological image (set to "1" or "on" to enable, or the default "0" or "off" to disable). "Bias" (on/off), when enabled, will sample all unequal pathways equally. "Scale" sets the scale for the images in microns per pixel. "Bc" sets the boundary conditions; options are buffer (default) and reflect. The conditions for stopping the simulation can be stopped in one or more of three different methods. "Ctme" sets the amount of time spent from the beginning of the simulation, "nrs" sets the number of capture reactions, and "clock" specifies an actual time/date to terminate the program. Finally, "nbins" sets the number of bins used in calculating microdosimetric parameter distributions. The order of the cards explained in this paragraph is irrelevant.

A blank line must separate the final portion of the input deck, the material cards. Each distinct region specified in the segmented image file (see next paragraph) is given a name in this section, followed by "tally", if results are to be tabulated in the region. If using a homogenous source distribution, "nosrc" will omit a region from containing sources. Materials may have any integer from 0 to 255. A blank line must follow the last material.

The other required input is a segmented image file outlining each structure of interest. Often, cell nuclei are considered an important target, so a typical strategy is to paint the cytoplasm and extracellular space one color (and, to save time, not tally results

in this region), while shading in nuclei with different colors. The actual colors used are not important; the file's look-up-table contains the important information.

The remaining two input files are optional. A track image, created in TrackAnalysis, can be supplied to give the locations of lithium-helium pair origins. Optionally, one may select a homogenous distribution in the input deck in lieu of a track image. The other elective file is a histological image. Its purpose is primarily to illustrate the charged particle tracks on a relevant background, using "mark" and "trace."

4.3 Microdosimetry Parameters

Once all the inputs are given, Boncres is ready to sample the source. The spatial distribution of sites is either provided by the user, or some uniform arrangement specified in the input deck. Two other pieces of information are determined by MATLAB's random number generator: particle directions and decay pathway. The exact details of the code's tracking algorithms are beyond the scope of this thesis, and are explained in Kiger's thesis. All parameters are given as two different averages: hit and event mean. Hit averages are tallied for a single event in a single object, while event means refer to all energy deposition from a single neutron interaction. One event can result in multiple hits, if the targets are tightly, bunched, or no hits, if all targets are missed.

The track length l is the total length of a particle track, inside a defined object of interest. Total particle track lengths are not precisely determined, due to range straggling, so stochastic measures are taken. A probability density function r for final particle ranges are integrated, and subtracted from one.

$$R(x) = 1 - \int_0^x r(x')dx'$$

and the track length is calculated by integrating the range cumulative density function R between the two intersection points with the object of interest, x_1 and x_2.

$$l = \int_{x_1}^{x_2} R(x)dx$$

Close to the origin of the track, $l = x_2 - x_1$. To speed up calculations, a cumulative track length function L is determined in the preprocessing phase by integrating

$$L(x) = \int_0^x R(x')dx'$$

and then determining l by simple subtraction

$$l = L(x_2) - L(x_1)$$

The energy imparted ε is the energy deposited in a target by charged particles from a neutron reaction. With x_1 and x_2 being the distances from the origin where the particle first hits, then terminates or leaves the target, respectively:

$$\varepsilon = \int_{x_1}^{x_2} LET(x)dx$$

Lineal energy y is defined as the average energy imparted divided by the mean chord length of the volume, intended to derive a value similar to LET. Because we simulate charged particle tracks, we can use the actual values for energy and track length, and calculate

$$y = \frac{\varepsilon}{\Delta x} = \frac{\int_{x_1}^{x_2} LET(x)dx}{\int_{x_1}^{x_2} dx}$$

The final calculated parameter is the dose weighted LET ζ, or DWLET. Proposed by Solares[3], it is an average LET, weighted by the LET itself.

$$\zeta = \frac{\int_{x_1}^{x_2} (LET(x))^2 dx}{\int_{x_1}^{x_2} LET(x) dx}$$

The intent of this value is to give an indication of the macroscopic effect expected, by taking advantage of the correlation between increasing LET and increasing biological effect. However, this parameter fails to take into account the peak in RBE at 100 kev/μm observed in most mammalian cells (figure 4.2), and is of limited practical value. An alternate parameter was suggested, using a weighting function to take into account the behavior seen in figure 4.2, but the variability between different cell types would make assembling such a parameter futile.

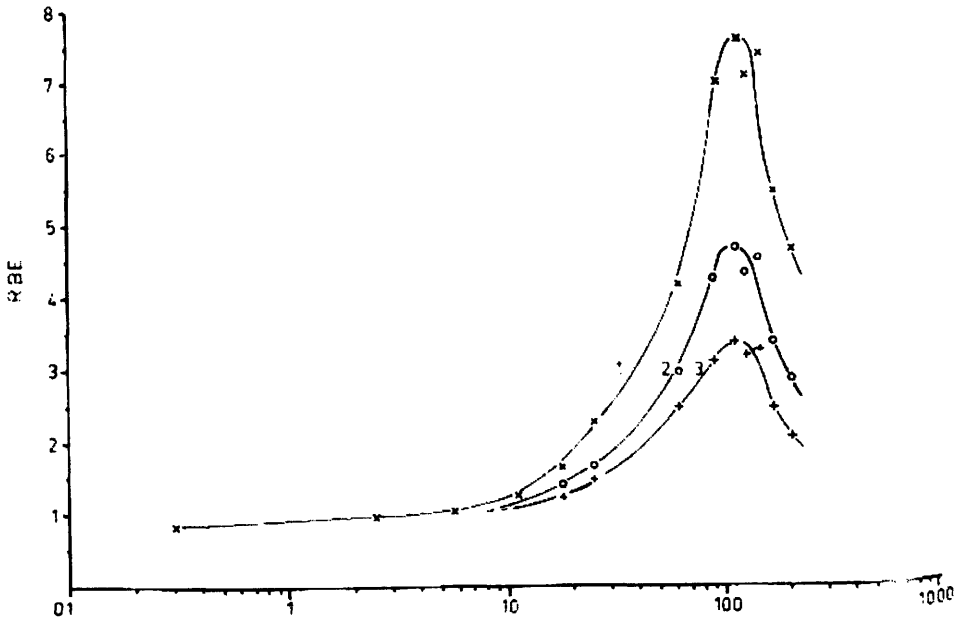

(Figure 4.2 Several RBE versus LET (kev/μm) curves[4])

In addition to calculating event and hit means of the above four parameters, other statistical figures are determined. Hit fraction, hit frequency, hit number distributions for

single events, and single event and hit probability distributions of the above four parameters are returned by Boncres.

4.4 Verification

Boncres was developed for MATLAB, which is a platform-independent development environment. Boncres, however, was coded in the late 1990's, on a power Macintosh, using MATLAB version 5.2.1. After updating the code to reflect changes in MATLAB version 7.1, and user interface considerations caused by switching to a Windows XP machine, there was no strong reason to suspect that the underlying calculation algorithms would be faulty. However, to be certain, we ran a string of test cases to verify that we could still have confidence in the simulation's calculated results.

The test cases are among those used by Kiger in his initial verification of Boncres. Some simplifications are made to create a problem in which the simulated parameters can be analytical determined as well, using geometric considerations. Range straggling is not allowed; the lithium ion always travels 4.2 μm and the alpha particle traverses 7.7 μm. The LET is a constant 400 kev/μm over the entire track length. Finally, the 6% probability of decay pathway to a ground state lithium nucleus is ignored.

A circular target is used, of area 100 pixels in Case A, and 200 pixels in Case B. A circular target is chosen for geometric simplicity, and the different pixel counts are used to ensure that resolution has minimal effect on results. The spatial scale of pixels to microns was set for four different physical lengths: 1/5, 1/2, 1, and 2 times the total track length of 11.9 μm. A homogenous source is employed, with source points in the target,

as well as an annulus surrounding the target allowing an alpha particle from as far away as 7.7 μm to strike the target. A buffer surrounds this annulus; by limiting the source in this fashion, one makes the simulation more efficient by filtering out events that have zero chance of scoring a hit. The analytical calculations for the simplified cases are omitted from this thesis.

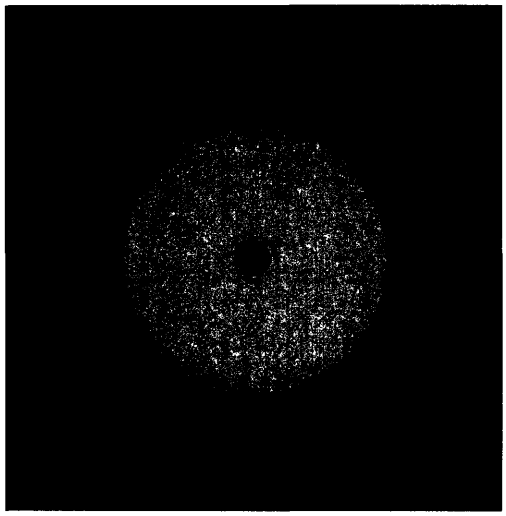

(Figure 4.3 Case1a. Center red circle is 100 pixels, and 1/5 of the 11.9 μm total track length, ~ 2.2 μm, in diameter, with an annulus allowing reactions up to 7.7 μm away.)

Each case was simulated with 1,000,000 events, and high resolution bins of 512 were employed, making statistical uncertainties in the parameters less than 1%. Correlation between simulation and analytically derived results was very good; all but one discrepancy was below 1%. The results are summarized in the table below.

		Hit Frequency					
D/T	Analytical	A	A std	A Error	B	B std	B Error
0.2	0.132	0.1328	0.0003	0.63%	0.1328	0.0003	0.63%
0.5	0.275	0.2781	0.0004	1.13%	0.2772	0.0004	0.79%
1	0.432	0.4350	0.0005	0.69%	0.4328	0.0005	0.19%
2	0.603	0.6063	0.0005	0.55%	0.6088	0.0005	0.96%

Hit mean energy imparted (MeV)

D/T	Analytical	A	A std	A Error	B	B std	B Error
0.2	0.647	0.642	0.0008	-0.77%	0.642	0.0008	-0.77%
0.5	1.343	1.332	0.0014	-0.82%	1.336	0.0014	-0.52%
1	2.095	2.084	0.0019	-0.53%	2.089	0.0020	-0.29%
2	2.910	2.895	0.0021	-0.52%	2.902	0.0021	-0.27%

Event mean energy imparted (MeV)

D/T	Analytical	A	A std	A Error	B	B std	B Error
0.2	0.085	0.086	0.0002	0.90%	0.086	0.0002	0.90%
0.5	0.370	0.370	0.0007	0.10%	0.370	0.0007	0.10%
1	0.904	0.907	0.0013	0.30%	0.905	0.0013	0.07%
2	1.755	1.755	0.0019	-0.01%	1.766	0.0019	0.64%

Hit mean track length (microns)

D/T	Analytical	A	A std	A Error	B	B std	B Error
0.2	1.617	1.605	0.0020	-0.74%	1.605	0.0020	-0.74%
0.5	3.358	3.330	0.0036	-0.83%	3.339	0.0035	-0.57%
1	5.238	5.211	0.0050	-0.52%	5.223	0.0050	-0.29%
2	7.274	7.236	0.0053	-0.52%	7.254	0.0052	-0.27%

Event mean track length (microns)

D/T	Analytical	A	A std	A Error	B	B std	B Error
0.2	0.213	0.213	0.0006	0.17%	0.2134	0.0006	0.17%
0.5	0.924	0.926	0.0018	0.21%	0.925	0.0018	0.10%
1	2.261	2.266	0.0034	0.23%	2.261	0.0034	0.00%
2	4.387	4.388	0.0048	0.02%	4.417	0.0048	0.67%

Event mean lineal energy (keV/micron)

D/T	Analytical	A	A std	A Error	B	B std	B Error
0.2	52.8	53.2	0.1421	0.82%	53.2	0.1422	0.82%
0.5	110.2	111.2	0.1878	0.92%	110.8	0.1876	0.55%
1	172.8	174.0	0.2077	0.70%	173.1	0.2075	0.17%
2	241.3	242.5	0.2063	0.50%	243.5	0.2061	0.93%

(Figure 4.3 Results of analysis versus simulations for test cases A and B)

Omitted are the hit means of lineal energy and DWLET which are, by definition of the conditions of the problem, constant at 400 kev/μm. The correspondence between analytically derived values and simulated results gives us confidence that the algorithm is accurate.

---

[1] Kiger III WS, "Developments in Micro- and Macro-Dosimetry of Boron Neutron Capture Therapy," Ph.D. Thesis, Massachusetts Institute of Technology, 2000.
[2] Yam CS, Zamenhof RG. "Computational Validation of the Stereology Principle Applied to the Microdosimetry of Boron Neutron Capture Therapy." *Med Phys.* Mar;27(3):549-557, 2000.
[3] Solares G, Kiger III WS, Zamenhof R, "Microdosimetry Studies at the Harvard/MIT Phase-I Clinical Trial of Boron Neutron Capture Therapy," in *Advances in Neutron Capture Therapy*, ed. Larsson B, Crawford J, Weinreich R, Elsevier, Amsterdam (1997).
[4] Hall EJ, Radiobiology for the Radiologist. 5th ed. Lippincott Williams & Wilkins; New York, 2000.

Chapter 5
BPA vs. MAC Therapeutic Comparison

5.1 Introduction

One of the challenges facing BNCT is the development of new, more efficacious boron delivery compounds. An ideal therapy compound: 1. has low system toxicity; 2. has high tumor uptake compared to normal tissue and blood; and 3. is rapidly cleared from normal tissue and blood, with tumor concentrations persisting throughout the neutron therapy.[1] HRQAR is ideally suited to testing the second requirement, as direct *ex vivo* boron concentration measurements are possible in different anatomical regions.

Modern clinical trials have been conducted with two different compounds, originally developed in the 1960's. [(L)-4-dihydroxy-borylphenylalanine], called BPA, is based on arylboronic acids; it is enriched with boron and complexed with fructose to improve water solubility.[2] The other, based on sodium mercaptoundecahydro-*closo*-dodecaborate, is called BSH.[3]

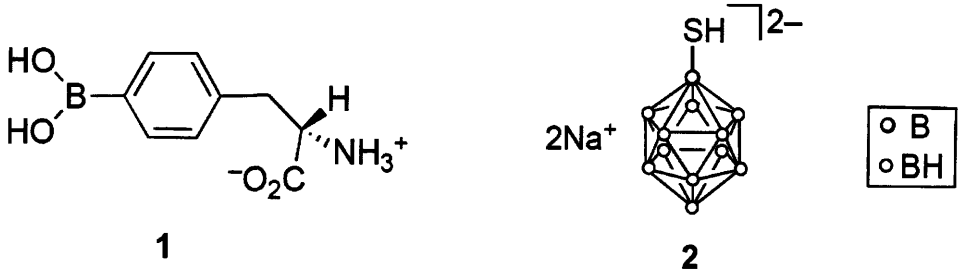

(Figure 5.1 BPA and BSH[1])

A newer class of compound being investigated utilizes liposomes for boron delivery. Liposomes have special properties due to their structure. They can encapsulate concentrated aqueous solutions of water-soluble polyhedral borane anion salts, and they can incorporate lipophilic boron-containing moieties within the bilayer membrane. Clearance time from the tumor increases, though the exact mechanism for this is not well understood.[4]

This experiment will compare the accumulation of boron in tumor of one of the clinically approved compounds, BPA, with that of an experimental liposomal compound K^+ [*nido*-7-$CH_3(CH_2)_{15}$-7,8-$C_2B_9H_{11}$]$^{1-}$ called MAC.

5.2 Procedure

EMT6 tumor cells were injected subcutaneously on the back of 5 BALB/c female mice, and allowed to grow for one week. After the tumors reached sizes ranging from 50-200 mm^3, two mice were injected with BPA 43mg ^{10}B/kg and sacrificed 6 hours later, two mice were injected with MAC 6mg ^{10}B/kg and sacrificed 30 hours later, and the fifth mouse was sacrificed to check background tracks and histology. This was repeated on a second batch of mice after the initial experiment. In addition, two additional mice were injected with a compound comprised of MAC with the fluorescent tag rhodamine DHPE.

On sacrifice, the tumor was removed and immediately frozen in liquid nitrogen. Samples were then placed in a -80 °C freezer for storage. 4 μm cryosections were placed on coated slides, as specified in Chapter 2. Samples were irradiated in the MIT-R thermal neutron beam with a fluence of 2.9×10^{13}, verified by gold foils. Standard

procedure for HRQAR staining and reversal were followed, and representative micropictographs were taken and analyzed. Boron-10 standards were also irradiated, and the resultant calibration curve is displayed below.

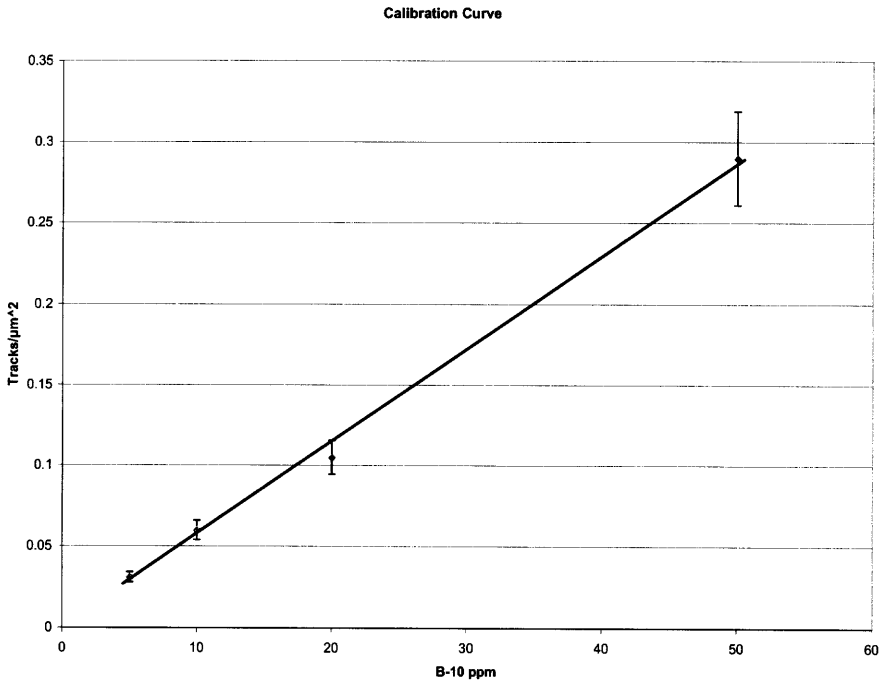

(Figure 5.2 B-10 calibration curve for this experiment)

5.3 Results

Initial, qualitative examination of the micropictographs revealed something startling: the liposomal compound accumulated almost exclusively on the surface of the tumor.

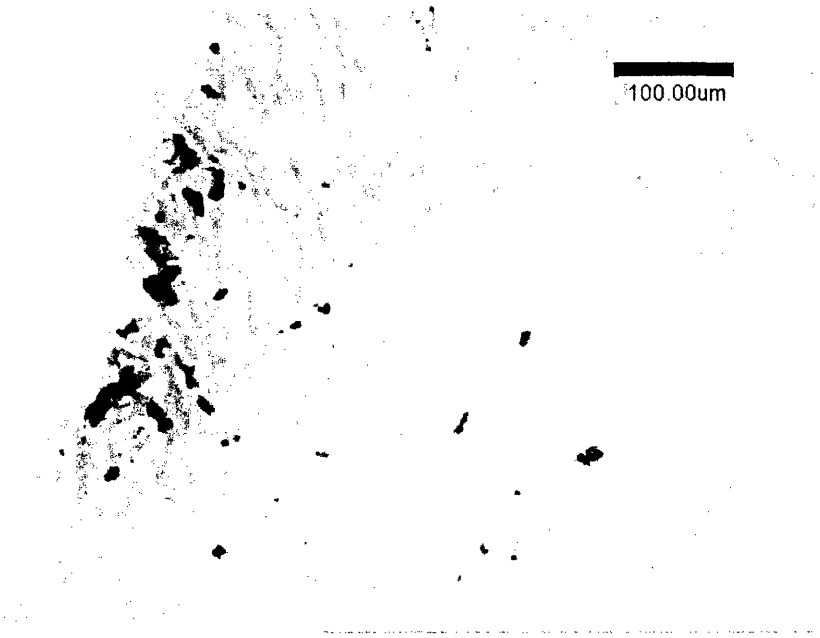

(Figure 5.3 Fluorescent tagged MAC in EMT6 tumor)

In Figure 5.3, the chrome colored areas correspond to fluorescence. The boundary of the tissue sample is visible on the left hand portion of the figure, and the fluorescence accumulates on the boundary, penetrating ~ 50 μm in. Isolated spots are visible in the interior as well. The fluorescent image, taken at 10X magnification, is useful in giving a

qualitative overview of what is happening; HRQAR is quantitative, but magnifications less than 40X make detecting tracks difficult.

HRQAR of the samples produced similar results. Images taken of the interior of the tumor show a track density no greater than background.

(Figure 5.4 EMT6 Interior with MAC. Tracks enhanced in Photoshop)

The boron compound appears unable to penetrate deeply into the tumor. Analysis of the tumor edge yielded data consistent with the fluorescent image.

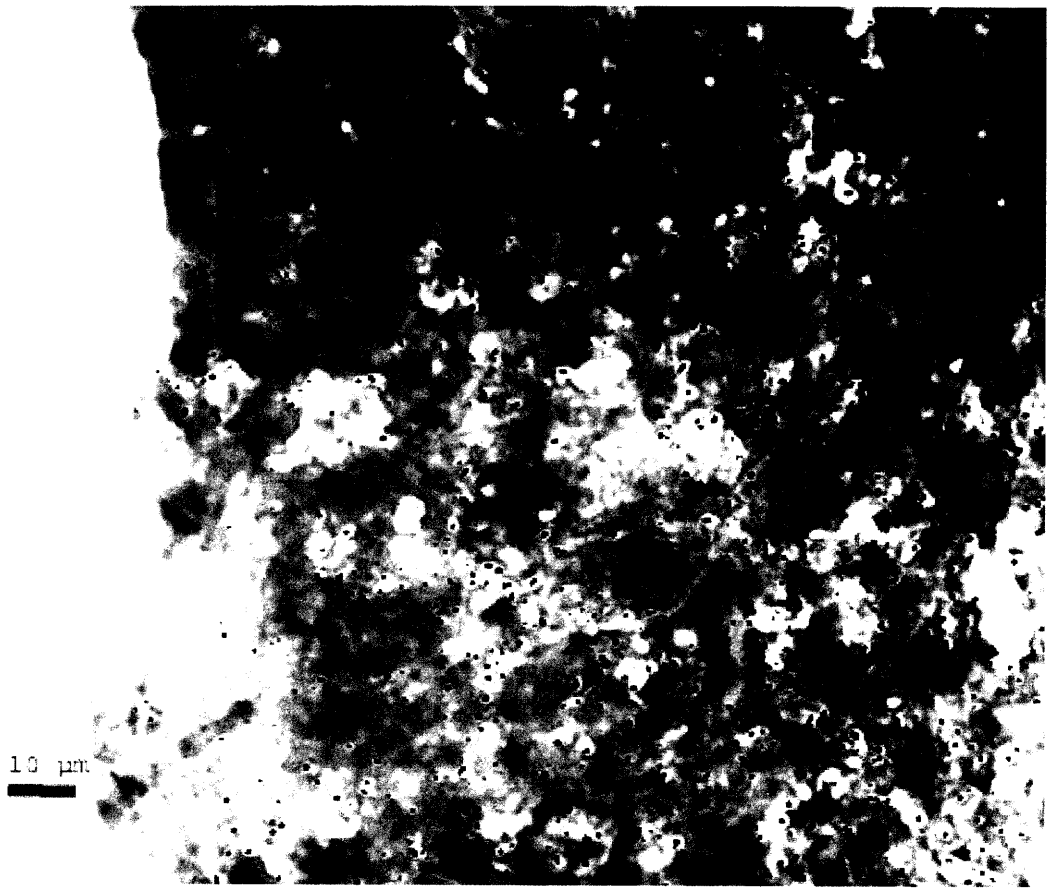

(Figure 5.5 Edge of EMT6 tumor with MAC. Tracks enhanced in Photoshop)

Boron concentrations at the edge fluctuated wildly, but were generally around 31.6 ppm, with a standard deviation of 16.7.

Analysis of mice injected with BPA yielded contrasting results. Tracks were present throughout the tumor, and the concentration fluctuations present were lower than with MAC.

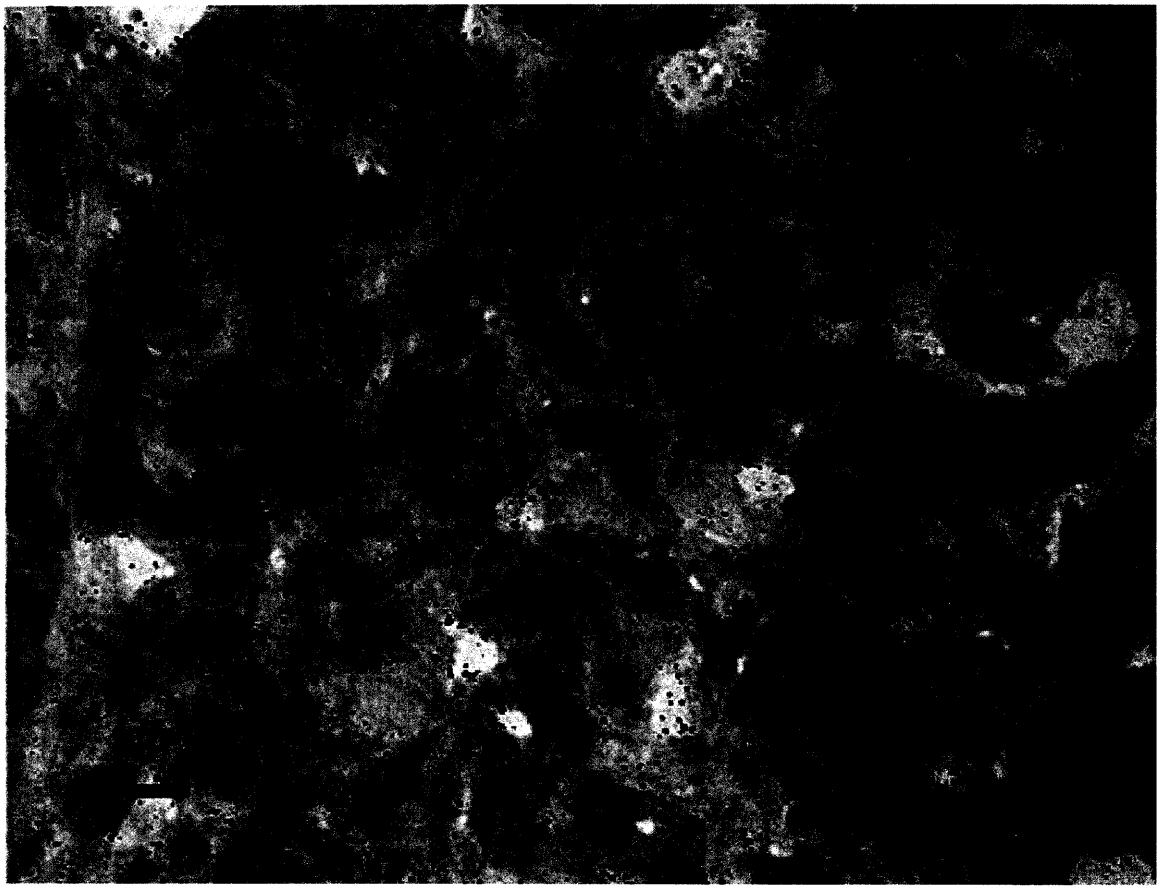

(Figure 5.6 EMT6 tumor with BPA. Tracks enhanced in Photoshop)

No correlation was found with location in tumor and boron concentration. Boron concentration was found to be 14.8 ± 3.1 ppm.

5.4 Analysis

The experiment shows that MAC is unlikely to be an improved boron compound for neutron capture therapy. MAC appears to lack the ability to diffuse fully into the gross tumor mass, leaving a significant number of cells unexposed to the heavy, energetic decay ions of the boron capture reaction.

One possible reason for the failure of MAC may be due to its diffusion behavior. The liposome does not diffuse into the surrounding tissue from the microvasculature.[5] (This behavior is also explored in Chapter 6 of this thesis.) If the center of the tumor is poorly vascularized, then little to no MAC would be present, which is the observed pattern.

In our laboratory, further experiments on MAC have been conducted. A colleague conducted tumor control experiments on the same cell line, mouse type, and boron compounds. Preliminary results support the observations made in HRQAR, that MAC is likely a poor candidate for neutron capture therapy. MAC + 4Gy thermal neutrons controlled 0/11 tumors, MAC + 6Gy thermal neutrons controlled 0/8, and MAC + 8Gy thermal neutrons controlled 1/8; BPA + 6Gy thermal neutrons controlled 5/8 tumors.[6] The gross ^{10}B concentrations in the tumor at the time of irradiation due to BPA and MAC were the same: ~ 13 ppm.

---

[1] Barth RF, Coderre JA, Vicente MG, Blue TE. "Boron Neutron Capture Therapy of Cancer: Current Status and Future Prospects." *Clinical Cancer Research,* 11(11), 3987-4002. Jun 1, 2005.
[2] Snyder HR, Reedy AJ, Lennarz WJ. "Synthesis of Aromatic Boronic Acids, Aldehydo Boronic Acids and a Boronic Acid Analog of Tyrosine." *J Am Chem Soc* 80:835-838, 1958.
[3] Soloway AH, Hatanaka H, Davis, MA. "Penetration of Brain and Brain Tumor. VII. Tumor-Binding Sulfhydryl Boron Compounds." *J Med Chem* 10:714, 1967.
[4] Feakes DA, Shelly K, Hawthorne MF. "Selective Boron Delivery to Murine Tumors by Lipophilic Species Incorporated in the Membranes of Unilamellar Liposome." *Proc Natl Acad Sci* Feb 28;92(5):1367-1370, 1995.
[5] Schuller BW, Binns PJ, Riley KJ, Ma L, Hawthorne MF, Coderre JA. "Selective irradiation of the vascular endothelium has no effect on the survival of murine intestinal crypt stem cells." *Proc Natl Acad Sci* Mar 7;103(10):3787-3792, 2006.
[6] Chung, Y. Personal communication, 2006.

Chapter 6
Verification of Mouse Gut Microvasculature Irradiation

6.1 Introduction

Chapter 5 details an experiment for which HRQAR is well suited – a comparison of relative therapeutic efficacy of different neutron capture therapy compounds – but other uses for the technique abound.

Gastrointestinal (GI) tract damage is a limiting factor in radiation treatments, as it can initiate GI syndrome; symptoms include diarrhea, dehydration, septic shock, and even death in severe cases. Primarily associated with abdominal irradiation, GI syndrome occurs following the sterilization of all crypt stem cells, located in the base of the villi that compose the intestinal epithelium.[1] There are two different theories as to the mechanism for crypt cell inactivation. The traditional explanation notes that rapid growth of the stem cells makes them more radiosensitive, pinning the cause on direct damage from radiation.[2] Recent research, however, suggests that apoptosis in the intestinal vascular endothelial cells may directly lead to GI syndrome. Deletion of the gene controlling endothelial cell apoptosis converts the cause of death from GI syndrome to bone marrow syndrome.[3]

To investigate this, one would need to selectively irradiate the vasculature, and observe any onset of GI syndrome. BNCT is a useful tool to accomplish this, given the short range of the alpha and lithium particle released. ^{10}B was incorporated into a liposomal compound MAC (K^+ [*nido*-7-$CH_3(CH_2)_{15}$-7,8-$C_2B_9H_{11}$]$^{1-}$) plus TAC ($[B_{20}H_{17}NH_3]^{3-}$) known not to leak from the vasculature into tissue. This allows delivery

of a higher dose to the vascular endothelial cells relative to other cell types, if the compound does, in fact, not leak into the tissue. To verify that no such leakage occurs during the experiments, HRQAR is employed.

6.2 Methods

MAC+TAC liposomes were administered to female BALB/c mice, sacrificed after 30 minutes. The 30 minute time point was determined as optimal by boron biodistribution studies. A portion of the small intestine was removed, cut into 0.5 cm segments, and placed upright in a plastic receptacle filled with Tissue-Tek optimal cutting compound. The receptacle was then embedded in dry ice to freeze, and then stored in a -80 °C freezer. Embedding the gut upright facilitated the next step: cryosectioning orthogonal cross sections of the intestines, so as to yield circular samples. Cryosections were placed on a coated quartz slide, and standard HRQAR procedures (Chapter 2) were employed.

6.3 Results

In order to verify that the vasculature is the target of our neutron capture irradiation, the vasculature must first be localized. Unfortunately, no vasculature staining technique has been tested for compatibility with HRQAR, but in this case, the gut microvasculature is fairly predictable. Figure 6.1 shows the results of staining using CD31 antigen. CD31 is a platelet endothelial cell adhesion molecule.

(Figure 6.1 Nuclei stained blue, vasculature is rust colored. The arrow in the left image points to a villus, the arrow in the right image points to a crypt.)

(Figure 6.2 Villus, with tracks from MAC+TAC in black, enhanced in Photoshop)

As shown in these images, the vasculature circles around crypts, and is confined to the interior of villi.

HRQAR images of BNCT tracks in the gut are consistent with locations known to contain microvasculature. Figure 6.2 above, for example, shows an image of a representative villus. The interior of the villus contains a high density of tracks, while the epithelial cells on the exterior exhibit only trace indications of potential liposomal compound leakage. HRQAR images of the crypts at the base of the villi show similar confirmation.

(Figure 6.3 Crypts, with tracks in black, enhanced in Photoshop)

A high density of tracks is present immediately surrounding the crypts, while the interiors display only trace evidence of leakage. It is difficult to quantify the blood boron concentration without uniting the CD31 antigen stain and the track images in one image. Because the cryosection is a planar cross section of the gut, the vasculature winds its way in and out of the plane, but rough calculations using only the small areas with high densities place it at ~ 110 ppm. The uncertain location of the vasculature limits the utility of that number. This is consistent with prompt gamma neutron activation analysis of the blood boron levels of 118 ± 12 ppm.

6.4 Conclusion

This experiment demonstrates a novel use for HRQAR: verification of selective irradiation of targets of interest. In this case, the goal was to irradiate the vascular endothelial cells, while sparing the crypts. HRQAR was able to demonstrate that a significantly higher amount of ^{10}B dose was delivered to areas serviced by intestinal microvasculature, relative to the crypts.

---

[1] Schuller BW, Binns PJ, Riley KJ, Ma L, Hawthorne MF, Coderre JA. "Selective irradiation of the vascular endothelium has no effect on the survival of murine intestinal crypt stem cells." *Proc Natl Acad Sci* Mar 7;103(10):3787-3792, 2006.

[2] Potten CS. "Radiation, the ideal cytotoxic agent for studying the cell biology of tissues such as the small intestine." *Radiation Research* Feb;161(2):123-136, 2004.

[3] Paris F, Fuks Z, Kang A, Capodieci, P, Juan G, Ehleiter D, Haimovitz-Friedman A, Cordon-Cardo C, Kolesnick R. "Endothelial apoptosis as the primary lesion initiating intestinal radiation damage in mice." *Science* Jul 13;293(5528):293-297, 2001.

Chapter 7
Conclusion and Future Directions

7.1 Conclusion

The practice of high resolution quantitative auto-radiography has been revived at MIT. Along the way, observations were made to increase the understanding of how to successfully perform HRQAR. These observations are spread throughout Chapter 2, but as an example: our experience with bubble formation in makrolon films dictated specific preparation, handling, and storage procedures for the fragile film, not previously known to be essential. In addition, modifications and improvements have made HRQAR more efficient and flexible. The time required to perform the procedure start-to-finish is now 2/3rds that of what it used to be. Furthermore, the irradiation procedure was adapted from the 3GV port to the medical thermal beam, allowing us to irradiate samples virtually on-demand.

The two software codes for image manipulation and analysis have been ported to the modern versions of MATLAB and Windows. Verification tests were performed after the conversion, in order to assure that the underlying algorithms survived the migration intact.

HRQAR was applied to two different experiments. Its primary purpose of assessing therapeutic efficacy was demonstrated in a comparison between BPA and a potential new liposomal compound MAC. Data from this experiment effectively explain the lower probability of tumor control observed with MAC. A novel use for HRQAR was also demonstrated in a mouse gut irradiation experiment. In conjunction with a

boronated compound believed to stay within the gut vasculature, boron neutron capture was used to selectively irradiate capillaries. HRQAR images corroborated that the capture reactions take place in the microvasculature.

HRQAR is working consistently, reliably, and reproducibly at MIT, and with the permanent staff trained in the procedure, it should continue assisting the development of boron neutron capture therapy into the future.

7.2 Future Work

Although the HRQAR process has been improved, and its success rate is high, there are issues that need to be addressed. Most pressing – and this was briefly mentioned in Chapter 2 – is the possibility of boron migration during a brief thaw. Traditionally, cryosections are placed onto a microscope slide, and then "melted" on, so that they adhere. In practice, this means placing the slide on a warm spot (the sectioner's gloved wrist, for example) for ~ 5 seconds. During this brief thaw, is it possible that the boron is displaced, negating HRQAR's claim of ~ 1-2 μm spatial resolution?

Referring to a standard biology textbook[1], a preliminary calculation does provide cause for concern. The diffusion coefficient is calculated by

$$D = \frac{2kT}{3\pi r \eta}$$

Using the following values:

k = 3.3 x 10^{-27} kcal/K (Boltzmann's constant)

T = 310 K (body temperature)

r = 2.5 nm = 2.5 x 10^{-3} μm (radius of phenylalanine, ie, BPA)

$\eta = 2.4 \times 10^{-11}$ kcal s/cm^3 = 2.4×10^{-23} kcal s/μm^3 (viscosity of interior of a cell)

one calculates a diffusion coefficient of

$$D = \frac{2(3.3\times10^{-27})(310)}{3\pi(2.5\times10^{-3})(2.4\times10^{-23})} = 3.618\frac{\mu m^2}{s}$$

The mean square displacement is calculated with:

$$\langle x^2 \rangle = q_i D t$$

where q_i is a dimensionless coefficient, and equal to 2, 4, or 6 for 1-D, 2-D, or 3-D situations, respectively. The time for BPA to diffuse 1 μm^2 is:

$$t = \frac{\langle x^2 \rangle}{q_i D} = \frac{1}{4(3.618)} = 0.069s$$

If this value is close to being true, then the five seconds the tissue spends thawing greatly reduces our spatial resolution. However, more factors than simple diffusion may be at work here, and this needs to be confirmed experimentally.

Designing an experiment to test this with HRQAR is difficult due to its stochastic nature. However, Chandra's group at Cornell, in their SIMS experiments, is able to keep their tissue samples at -80 °C from start to finish, by using special indium substrate for adhering the tissue.[2] By maintaining such low temperatures, the liquid interior of a cell, which is composed primarily of water, will be solid at all times. Viscosity is a property of fluids and gases, but one can think of solids as being highly viscous fluids; *D* would be correspondingly quite small at -80 °C, making the time *t* to migrate 1 μm quite large. Mazur reports that diffusion times would be on the order of years.[3] Using Chandra's preparation technique, one can perform an experiment where one varies the time spent at different temperatures warmer than -80 °C from zero seconds, up to an hour (about the

maximum time spent out of the freezer during neutron irradiation) to chart the effect of different thaw durations on boron mobility, using SIMS before-and-after images. If the brief thaw is a problem, the next step will be adopting a new sample preparation technique that does not involve any thawing. Using an indium substrate would be one such solution.

Improvements to sample preparation beyond temperature controls also require further investigation. Sectioning frozen tissue into thin slices is difficult, and microscopic fragmentation is not unusual, making portions unusable for HRQAR analysis. Additional tissue stains should be investigated, and their compatibility with the fragile polymers used assessed. We encountered points in our experiments where staining for vasculature would have been informative, such as in the experiment described in Chapter 6, for example. Finally, the image acquisition and analysis process involves considerable human input, and is time-consuming. Any way to help automate the process will be of great help to future researchers wanting to employ HRQAR. Developing a software routine that can function as an "auto-focus" would considerably ameliorate the time-consuming and tedious process, and lead to automatic imaging of an entire sample via macros, with little user input.

---

[1] Lodish, et. al. Molecular Cell Biology 3rd ed. Scientific American Books: New York, 1999.
[2] Chandra S, Smith DR, Morrison GH. "Subcellular Imaging by Dynamic SIMS Microscopy." *Analytical Chemistry* Feb 1; 72(3):104A-114A, 2000.
[3] Mazur, P. "Freezing of Living Cells: Mechanisms and Implications." *Am J Physiol Cell Physiol* 247:C125-C142, 1984.

Appendix A
HRQAR Procedure Outline

This appendix assumes that the reader is familiar with HRQAR, and has successfully performed it in the past. The intent is to provide a concise reference for the order of steps, and if more information is needed, refer to Chapter 2.

1. Polymer coatings
    a. Apply makrolon coating to clean quartz slide; Color should be blue/purple
        i. Allow 24 hours to dry
    b. Apply ixan coating over makrolon; use yellow/red regions
        i. Allow 6 hours to dry
    c. Apply second ixan coating
        i. Allow 6 hours to dry
    d. Laminate in Petri dish with dichloromethane for 40 seconds
        i. Store slides in -80 °C freezer
2. Cryosectioning
    a. Set working temperature to ~ -20 °C
    b. Aim for no thicker than 4 μm sections
    c. Fix tissue to polymers by briefly "melting" it using a heat source
3. Thermal Neutron Irradiation
    a. Keep tissue as cold as possible throughout
    b. Use gold foils and/or boric acid standards for benchmarks

c. Adjust fluence based on expected boron concentrations to avoid problems with track saturation or sparse track statistics

d. Allow 1-2 days for ^{31}Si isotope to decay

4. Hematoxylin & Eosin Staining

a. Allow tissue to come to room temperature

b. Have glycerol/gelatin mountant warming in a 55 °C water bath

c. Follow staining steps outlines in Chapter 2.8

d. Immediately after staining, proceed to mounting

5. Mounting

a. Place 5-6 drops of mountant on polymer and tissue

b. Orient cleaned glass slide anti-parallel to quartz, such that slides overlap entire polymer/tissue region

i. Squeeze firmly to remove any air bubbles in mountant

c. Place in 4 °C refrigerator for 2-3 days

6. Reversal

a. Scrape excess mountant from edges of slides

b. Apply firm, mutually opposed torques on the slide handles

i. Do not gradually apply force, but do not forcibly handle them either

c. Scrape the quartz slide with a razor to verify full transfer of polymers

7. Etching

a. On slides, paint areas not near tissue with ixan

i. Allow 15 minutes to dry

b. Apply second ixan painting
    i. Allow 15 minutes to dry
c. Mix etchant according to Chapter 2.11
    i. Exothermic reaction; either allow sufficient time for solution to return to room temperature, or place in water bath
d. Immerse slides in etchant for 30-40 minutes
e. Rinse with 47% ethanol, set aside to dry

Appendix B
Reagent Recipes

Makrolon Solution

3. Makrolon resin 42.4g
4. Dichloromethane 487.6g

Dissolve resin in dichloromethane, and lightly stir until fully dissolved.

Ixan Solution

1. Ixan Resin 12.6 g
2. n-Butylacetate 30.0 g
3. Trichloroethylene 57.9 g
4. Cyclohexanone 0.8 g
5. Dibutylphthalate 1.6 g

Mix ixan resin in the n-butylacetate, stir until fully dissolved (at least 6 hours). Color is dark yellow. Add trichloroethylene, stir for 24 hours. Filter using Millipore polypropylene prefilter (type AN12, catalog # AN1204700). Add cyclohexanone and dibutylphthalate, stir for 24 hours.

Harris Hematoxylin

1. Harris Hematoxylin 100 ml
2. Glacial Acetic Acid 2-4 ml

Mix and filter before using. Color should be deep purple

1% Eosin Stock

1. Eosin Y, Water Soluble 1.0 g
2. Distilled Water 20 ml
3. 95% Alcohol 80 ml

Dissolve eosin completely in water, then add alcohol and stir. Color should be an iridescent orange.

Working Eosin Solution

1. 1% Eosin Stock 1 part
2. 80% Alcohol 3 parts
3. Glacial Acetic Acid 0.5 ml/per 100 ml

Just before use, dissolve stock eosin in alcohol, then add acetic acid and stir. Color should be brilliant orange.

Acid Alcohol

1. 70% Alcohol 100 ml
2. Hydrochloric Acid 1 ml

Mix and stir.

Ammonia Water

1. Tap Water 500 ml
2. 28% Ammonium Hydroxide 1 ml

Mix and stir.

Lithium Carbonate

1. Lithium Carbonate 1 g
2. Distilled Water 100 ml

Mix and stir.

Etching Solution

1. KOH Pellets 9 g
2. Distilled Water 27 g
3. 100% Ethanol 24 g

Dissolve KOH in water, cover with parafilm, and stir. Add ethanol, recover, and stir.